Cost-Effective Bypass Design of Highly Controllable Heat-Exchanger Networks

Q. Z. Yan, Y. H. Yang, and Y. L. Huang
Dept. of Chemical Engineering and Materials Science, Wayne State University, Detroit, MI 48202

Design of a cost-effective and highly controllable heat-exchanger network (HEN) has drawn a great deal of attention for years. One of the key issues in such a design is how to effectively minimize undesirable disturbance propagation in a network with minimum cost increment. Design options in this regard include the derivation of a superior network structure and the selection of bypasses associated with heat exchangers. A unique system modeling approach is developed to predict disturbance propagation and to reject disturbances using bypasses. A novel mathematical representation scheme for a HEN is introduced to facilitate system analysis and design. A relative gain-array approach is extended to the analysis of nonsquared systems. In addition, an iterative design procedure is introduced to determine optimal bypass locations and nominal fractions for complete disturbance rejection, while economic penalty reaches the minimum. The efficacy of the model-based approach is demonstrated by designing three HENs where bypasses are optimally placed, and the control schemes are simultaneously developed.

Introduction

A heat-exchanger network (HEN) always experiences various disturbances of temperatures and heat-capacity flow rates in operation. These disturbances propagate through the network that may make the control of stream output temperatures extremely difficult, if the network is improperly designed. Consequently, how to effectively reject disturbances through developing a superior HEN with optimally placed bypasses becomes a challenging task.

Over the past decade, disturbance propagation (DP) and disturbance rejection (DR) in processes have been extensively studied. A great deal of effort has been made to control DP for improving flexibility (Morari, 1983; Floudas and Grossmann, 1986; Calandranis and Stephanopoulos, 1986; Galli and Cerda, 1991). Flexibility is a system's capability of absorbing long-term variations appearing at the inlets of the process (Kotjabasakis and Linnhoff, 1986; Colberg and Morari, 1988; Yee and Grossmann, 1990; Papalexandri and Pistikopoulos, 1994b). In contrast, controllability is referred to the system's capability of withstanding short-term disturbances. Morari (1992) pointed out that HEN controllability is largely dependent upon its network structure. Clearly, controllability analysis should be an integral part of process design. More appropriately, it should be referred to the analysis of structural controllability that focuses on the structural property of a process.

To ensure structural controllability, Calandranis and Stephanopoulos (1988) proposed an approach to the design of control loops for a HEN and to sequence the control actions of the loops in order to accommodate setpoint changes and to reject load disturbances. From the process design point of view, Fisher et al. (1988a,b,c) introduced a systematic procedure for assessing process controllability, where control-related economic penalties could be imposed in process screening. Mathisen et al. (1991) considered the dynamic resilience of a HEN based on the notion of static resilience that was introduced by Saboo et al. (1985). Later on, Mathisen et al. (1992) provided a heuristic method for bypass placement. The resultant HEN is supposedly satisfactory in rejecting disturbances over a moderate range of operating conditions. Papalexandi and Pistikopoulos (1994a,b) introduced a systematic framework for the synthesis or retrofit of a flexible and structurally controllable HEN. Dynamic controllability of a HEN was considered using a hyperstructure network repre-

Correspondence concerning this article should be addressed to Y. L. Huang.

sentation scheme. A cost-effective network with favorable control scheme could be derived using MINLP. Uzturk and Akman (1997) described an MINLP method for optimal retrofit design of a HEN with bypasses. Aguilera and Marchetti (1998) developed a procedure for on-line optimization and control system design of a HEN also using MINLP.

More recently, Yang et al. (1996, 1999, 2000) introduced a unique modeling approach to quantify DP in a HEN, a MEN, and a distillation column network (DCN) at the steady-state level. By that approach, a system DP model can be developed based on the first principles. The model can be used to quickly estimate the maximum deviation of system outputs when it experiences the worst combination of various types of disturbances. The estimation precision is satisfactory enough in industrial applications. The model is linear and applicable to a network of any complexity. The modeling approach shows its great potential in being embedded into a process synthesis procedure (Yang et al., 1999). However, the DP models do not contain the term representing feasible, necessary control actions for DR. This can lead to a conservative network design.

This article is the first to extend Yang's DP model to a disturbance propagation and control (DP&C) model. The new system model will characterize the system behavior under control. The model is then embedded into a design procedure for optimally selecting bypasses that includes their locations and nominal fractions, with the minimum penalty on capital cost. Furthermore, the design procedure will suggest the most desirable control schemes for complete DR in the network.

Simplified Disturbance Propagation Model Without Bypass

Yang et al. (1996) developed a first-principles-based DP model for a heat exchanger (HEX) without bypass. By neglecting high-order differentiation terms and replacing a logarithmic mean temperature difference by an arithmetic mean term, the model can be simplified to a linear one as follows:

$$\boldsymbol{\delta T^t = D_t \delta T^s + D_m \delta Mc_P} \tag{1}$$

or

$$\begin{pmatrix} \delta T_h^t \\ \delta T_c^t \end{pmatrix} = \begin{pmatrix} 1-\alpha & \alpha \\ \beta & 1-\beta \end{pmatrix} \begin{pmatrix} \delta T_h^s \\ \delta T_c^s \end{pmatrix} + \begin{pmatrix} \alpha_h(2-\alpha) & -\alpha_c\alpha \\ \alpha_h\beta & -\alpha_c(2-\beta) \end{pmatrix} \begin{pmatrix} \delta Mc_{P_h} \\ \delta Mc_{P_c} \end{pmatrix}, \tag{2}$$

where

$$\alpha = \frac{T_h^s - T_h^t}{T_h^s - T_c^s} \tag{3}$$

$$\beta = \frac{T_c^t - T_c^s}{T_h^s - T_c^s} \tag{4}$$

$$\alpha_h = \frac{T_h^s - T_h^t}{2Mc_{P_h}} \tag{5}$$

$$\alpha_c = \frac{T_c^t - T_c^s}{2Mc_{P_c}}. \tag{6}$$

The preceding model can be used to provide a quick and accurate quantification of DP through a HEX. This greatly facilitates the analysis of DP-focused structural controllability in the early stages of HEN design (Yang, 1999).

Disturbance Propagation and Control Model

In operation, a HEN is always controlled through regulating bypass flow rates associated with HEXs. This requires the extension of the DP model by Yang et al. (1996) to a DP&C model where control actions are taken into account.

Unit-based model

A HEX with bypass options is sketched in Figure 1. The energy balance and heat-transfer equations can be readily derived, as below. Here, an arithmetic mean-temperature difference is used. This approximation will not introduce any calculation error for stream target temperatures when input temperature disturbances exist, but will cause some prediction errors when mass flow rate disturbances enter the system. Practically, bypass fractions will not be very significant, as shown in various practical examples; otherwise, a cost increment of relevant HEXs must be considerable.

$$Mc_{p_h} T_h^t = Mc_{p_h}^b T_h^s + Mc_{p_h}^e T_h^o \tag{7}$$

$$Mc_{p_c} T_c^t = Mc_{p_c}^b T_c^s + Mc_{p_c}^e T_c^o \tag{8}$$

$$Q = UA\frac{\left(T_h^i - T_c^o\right) + \left(T_h^o - T_c^i\right)}{2} = Mc_{p_h}^e\left(T_h^i - T_h^o\right) = Mc_{p_c}^e\left(T_c^o - T_c^i\right) \tag{9}$$

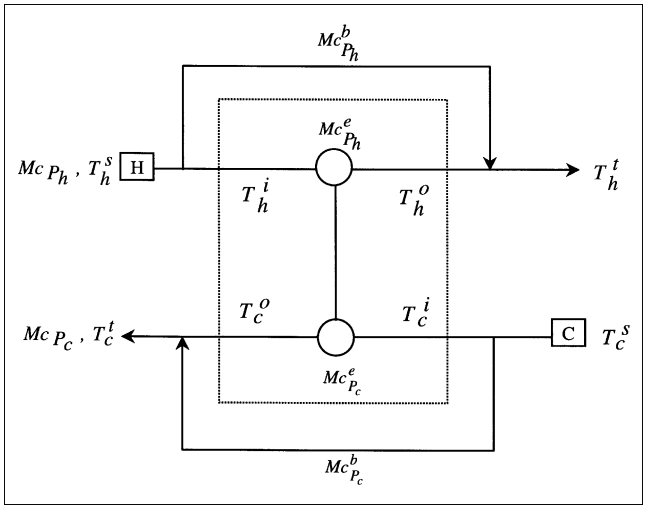

Figure 1. General structure of a heat exchanger with bypasses.

Since stream splitting does not change stream temperatures, T_h^i and T_c^i are equal to T_h^s and T_c^s, respectively. The mass flow rates in the two bypasses, $Mc_{p_h}^b$ and $Mc_{p_c}^b$, are equal to $f_h Mc_{p_h}$ and $f_c Mc_{p_c}$, respectively, where f_h are f_c are bypass fractions. When the model in Eq. 1 is applied to the inner part of the HEX (see the dotted box in Figure 1), the terms α, β, α_h, and α_c, in Eqs. 3 through 6 should be modified and are renamed below:

$$\alpha' = \frac{T_h^i - T_h^o}{T_h^i - T_c^i} = \frac{T_h^s - \dfrac{T_h^t - f_h T_h^s}{1-f_h}}{T_h^s - T_c^s} = \frac{T_h^s - T_h^t}{(1-f_h)(T_h^s - T_c^s)} = \frac{\alpha}{1-f_h} \quad (10)$$

$$\beta' = \frac{T_c^o - T_c^i}{T_h^i - T_c^i} = \frac{\dfrac{T_c^t - f_c T_c^s}{1-f_c} - T_c^s}{T_h^s - T_c^s} = \frac{T_c^t - T_c^s}{(1-f_c)(T_h^s - T_c^s)} = \frac{\beta}{1-f_c} \quad (11)$$

$$\alpha_h' = \frac{T_h^i - T_h^o}{2Mc_{p_h}^e} = \frac{T_h^i - T_h^o}{2(1-f_h)Mc_{p_h}} = \frac{T_h^s - T_h^t}{2(1-f_h)^2 Mc_{p_h}} = \frac{\alpha_h}{(1-f_h)^2} \quad (12)$$

$$\alpha_c' = \frac{T_c^o - T_c^i}{2Mc_{p_c}^e} = \frac{T_c^o - T_c^i}{2(1-f_c)Mc_{p_c}} = \frac{T_c^t - T_c^s}{2(1-f_c)^2 Mc_{p_c}} = \frac{\alpha_c}{(1-f_c)^2}. \quad (13)$$

Correspondingly, the model in Eq. 2 is modified as

$$\begin{pmatrix} \delta T_h^o \\ \delta T_c^o \end{pmatrix} = \begin{pmatrix} 1-\alpha' & \alpha' \\ \beta' & 1-\beta' \end{pmatrix} \begin{pmatrix} \delta T_h^s \\ \delta T_c^s \end{pmatrix} + \begin{pmatrix} \alpha_h'(2-\alpha') & -\alpha_c'\alpha' \\ \alpha_h'\beta' & -\alpha_c'(2-\beta') \end{pmatrix} \begin{pmatrix} \delta Mc_{p_h}^e \\ \delta Mc_{p_c}^e \end{pmatrix}. \quad (14)$$

Vectors $(\delta T_h^o \ \delta T_c^o)^T$ and $(\delta Mc_{p_h}^e \ \delta Mc_{p_c}^e)^T$ in the preceding model should be converted to $(\delta T_h^t \ \delta T_c^t)^T$ and $(\delta Mc_{p_h} \ \delta Mc_{p_c})^T$, respectively. Note that

$$\delta Mc_{p_h}^e = \delta\left((1-f_h)Mc_{p_h}\right) = -Mc_{p_h}\delta f_h + (1-f_h)\delta Mc_{p_h}. \quad (15)$$

Similarly,

$$\delta Mc_{p_c}^e = -Mc_{p_c}\delta f_c + (1-f_c)\delta Mc_{p_c}. \quad (16)$$

These two equations can be written in the following matrix form.

$$\begin{pmatrix} \delta Mc_{p_h}^e \\ \delta Mc_{p_c}^e \end{pmatrix} = \begin{pmatrix} -Mc_{p_h} & 0 \\ 0 & -Mc_{P_c} \end{pmatrix} \begin{pmatrix} \delta f_h \\ \delta f_c \end{pmatrix} + \begin{pmatrix} 1-f_h & 0 \\ 0 & 1-f_c \end{pmatrix} \begin{pmatrix} \delta Mc_{P_h} \\ \delta Mc_{P_c} \end{pmatrix}. \quad (17)$$

On the other hand, according to Eq. 7, we have

$$T_h^t = f_h T_h^s + (1-f_h)T_h^o. \quad (18)$$

Its differentiation gives

$$\delta T_h^t = T_h^s \delta f_h + f_h \delta T_h^s - T_h^o \delta f_h + (1-f_h)\delta T_h^o. \quad (19)$$

From Eqs. 18 and 19, we can have

$$\delta T_h^o = \frac{1}{1-f_h}\delta T_h^t - \frac{T_h^s - T_h^t}{(1-f_h)^2}\delta f_h - \frac{f_h}{1-f_h}\delta T_h^s. \quad (20)$$

Similarly,

$$\delta T_c^o = \frac{1}{1-f_c}\delta T_c^t - \frac{T_c^t - T_c^s}{+(1-f_c)^2}\delta f_c - \frac{f_c}{1-f_c}\delta T_c^s. \quad (21)$$

In matrix form, Eqs. 20 and 21 can be written as

$$\begin{pmatrix} \delta T_h^o \\ \delta T_c^o \end{pmatrix} = \begin{pmatrix} \dfrac{1}{1-f_h} & 0 \\ 0 & \dfrac{1}{1-f_c} \end{pmatrix} \begin{pmatrix} \delta T_h^t \\ \delta T_c^t \end{pmatrix} - \begin{pmatrix} \dfrac{T_h^s - T_h^t}{(1-f_h)^2} & 0 \\ 0 & \dfrac{T_c^t - T_c^s}{(1-f_c)^2} \end{pmatrix} \begin{pmatrix} \delta f_h \\ \delta f_c \end{pmatrix} - \begin{pmatrix} \dfrac{f_h}{1-f_h} & 0 \\ 0 & \dfrac{f_c}{1-f_c} \end{pmatrix} \begin{pmatrix} \delta T_h^s \\ \delta T_c^s \end{pmatrix}. \quad (22)$$

Substituting Eqs. 17 and 22 into Eq. 14 and simplifying it by using the relationships in Eqs. 10 through 13, we can obtain the following model:

$$\boldsymbol{\delta T^t = B\delta f + D_t \delta T^s + D_m \delta Mc_P}, \quad (23)$$

where

$$\boldsymbol{\delta T^t} = \left(\delta T_h^t \ \delta T_c^t\right)^T \quad (24)$$

$$\boldsymbol{\delta f} = \left(\delta f_h \ \delta f_c\right)^T \quad (25)$$

$$\boldsymbol{\delta T^s} = \left(\delta T_h^s \ \delta T_c^s\right)^T \quad (26)$$

$$\boldsymbol{\delta Mc_P} = \left(\delta Mc_{P_h} \ \delta Mc_{P_c}\right)^T \quad (27)$$

$$\boldsymbol{B} = \begin{pmatrix} \dfrac{\alpha\left(T_h^s - T_h^t\right)}{2(1-f_h)^2} & \dfrac{\beta\left(T_h^s - T_h^t\right)}{2(1-f_c)^2} \\ -\dfrac{\alpha\left(T_c^t - T_c^s\right)}{2(1-f_h)^2} & -\dfrac{\beta\left(T_c^t - T_c^s\right)}{2(1-f_c)^2} \end{pmatrix} \quad (28)$$

$$\boldsymbol{D}_t = \begin{pmatrix} 1-\alpha & \alpha \\ \beta & 1-\beta \end{pmatrix} \tag{29}$$

$$\boldsymbol{D}_m = \begin{pmatrix} \alpha_h\left(2-\dfrac{\alpha}{1-f_h}\right) & -\dfrac{\alpha\alpha_c}{1-f_c} \\ \dfrac{\beta\alpha_h}{1-f_h} & -\alpha_c\left(2-\dfrac{\beta}{1-f_c}\right) \end{pmatrix}. \tag{30}$$

The model in Eq. 23, named the unit-based DP&C model, is more general than the DP model in Eq. 1. In fact, if no bypass is involved (that is, f_h and f_c are equal to zero and thus δf_h and δf_c are zero), then the two models are identical.

System DP&C model

The unit-based DP&C model in Eq. 23 is applicable to any HEX in a HEN. That is, the model for the ith HEX, named E_i, in a network can be rewritten as

$$\boldsymbol{\delta T}_{E_i}^{\text{out}} = \boldsymbol{B}_{E_i}\boldsymbol{\delta f}_{E_i} + \boldsymbol{D}_{t_{E_i}}\boldsymbol{\delta T}_{E_i}^{\text{in}} + \boldsymbol{D}_{m_{E_i}}\boldsymbol{\delta Mc}_{P_{E_i}}. \tag{31}$$

If a HEN contains N_e heat exchangers, a system model can be obtained directly by lumping all unit-based models in the sequence of exchanger numbers. This yields

$$\boldsymbol{\delta T}^{*\,\text{out}} = \boldsymbol{B}_E^*\boldsymbol{\delta f}^* + \boldsymbol{D}_{t_E}^*\boldsymbol{\delta T}^{*\,in} + \boldsymbol{D}_{m_E}^*\boldsymbol{\delta Mc}_p^*, \tag{32}$$

where

$$\boldsymbol{\delta T}^{*\,\text{in}} = \left(\left(\boldsymbol{\delta T}_{E_1}^{\text{in}}\right)^T\left(\boldsymbol{\delta T}_{E_2}^{\text{in}}\right)^T\cdots\left(\boldsymbol{\delta T}_{E_{N_e}}^{\text{in}}\right)^T\right)^T \tag{33}$$

$$\boldsymbol{\delta T}^{*\,\text{out}} = \left(\left(\boldsymbol{\delta T}_{E_1}^{\text{out}}\right)^T\left(\boldsymbol{\delta T}_{E_2}^{\text{out}}\right)^T\cdots\left(\boldsymbol{\delta T}_{E_{N_e}}^{\text{out}}\right)^T\right)^T \tag{34}$$

$$\boldsymbol{\delta Mc}_p^* = \left(\left(\boldsymbol{\delta Mc}_{p_{E_1}}\right)^T\left(\boldsymbol{\delta Mc}_{p_{E_2}}\right)^T\cdots\left(\boldsymbol{\delta Mc}_{p_{E_{N_e}}}\right)^T\right)^T \tag{35}$$

$$\boldsymbol{\delta f}^* = \left(\left(\boldsymbol{\delta f}_{E_1}\right)^T\left(\boldsymbol{\delta f}_{E_2}\right)^T\cdots\left(\boldsymbol{\delta f}_{E_{N_2}}\right)^T\right)^T \tag{36}$$

$$\boldsymbol{B}_E^* = \mathbf{diag}\left\{\boldsymbol{B}_{E_1}, \boldsymbol{B}_{E_2}, \cdots, \boldsymbol{B}_{E_{N_e}}\right\} \tag{37}$$

$$\boldsymbol{D}_{t_E}^* = \mathbf{diag}\left\{\boldsymbol{D}_{t_{E_1}}, \boldsymbol{D}_{\mathbf{L}_{E_2}}, \ldots, \boldsymbol{D}_{t_{E_{Ne}}}\right\} \tag{38}$$

$$\boldsymbol{D}_{m_E}^* = \mathbf{diag}\left\{\boldsymbol{D}_{m_{E_1}}, \boldsymbol{D}_{m_{E_2}}, \ldots, \boldsymbol{D}_{m_{E_{N_e}}}\right\}. \tag{39}$$

The dimensions of vectors $\boldsymbol{\delta T}^{*\,\text{in}}$, $\boldsymbol{\delta T}^{*\,\text{out}}$, $\boldsymbol{\delta f}^*$, and $\boldsymbol{\delta Mc}_P^*$ are all $2N_e\times 1$, and those of matrices $\boldsymbol{B}_E^*$, $\boldsymbol{D}_{t_E}^*$, and $\boldsymbol{D}_{m_E}^*$ are all $2N_e\times 2N_e$. Note that $\boldsymbol{\delta T}^{*\,\text{in}}$ and $\boldsymbol{\delta T}^{*\,\text{out}}$ contain a total of N_m intermediate temperatures. An intermediate temperature is that of a stream between two adjacent HEXs. The term, N_m, can be evaluated as

$$N_m = 2N_e - N_s - N_{\text{split}}, \tag{40}$$

where N_e is the number of heat exchangers; N_s is the total number of hot streams (N_h) and cold streams (N_c); and N_{split} is the total number of stream branches after splitting. The preceding vectors can be reorganized in the following manner.

$$\boldsymbol{\delta \underline{T}}^{\text{in}} = \left(\delta T_{h_1}^s\cdots\delta T_{h_{N_h}}^s\delta T_{c_1}^s\cdots\delta T_{c_{N_c}}^s\delta T_1^m\cdots\delta T_{N_m}^m\right)^T = \left(\left(\boldsymbol{\delta \underline{T}}^s\right)^T\left(\boldsymbol{\delta \underline{T}}^m\right)^T\right)^T \tag{41}$$

$$\boldsymbol{\delta \underline{T}}^{\text{out}} = \left(\delta T_{h_1}^t\cdots\delta T_{h_{N_h}}^t\delta T_{c_1}^t\cdots\delta T_{c_{N_c}}^t\delta T_1^m\cdots\delta T_{N_m}^m\right)^T = \left(\left(\boldsymbol{\delta \underline{T}}^t\right)^T\left(\boldsymbol{\delta \underline{T}}^m\right)^T\right)^T. \tag{42}$$

In $\boldsymbol{\delta Mc}_P^*$, there are N_m redundant heat-capacity flow rates that should be eliminated. This reduces $\boldsymbol{\delta Mc}_P^*$ to $\boldsymbol{\delta Mc}_P$ [$(2N_e - N_m)\times 1$]. Correspondingly, $\boldsymbol{B}_E^*$, $\boldsymbol{D}_{t_e}^*$, and $\boldsymbol{D}_{m_E}^*$ should be changed in the following way:

$$\underline{\boldsymbol{D}_t^*} = \begin{pmatrix} \boldsymbol{D}_{t_{11}} & \boldsymbol{D}_{t_{12}} \\ \boldsymbol{D}_{t_{21}} & \boldsymbol{D}_{t_{22}} \end{pmatrix} = \boldsymbol{V_1}\boldsymbol{D}_{t_E}^*\boldsymbol{V_2} \tag{43}$$

$$\underline{\boldsymbol{D}_m^*} = \begin{pmatrix} \boldsymbol{D}_{m_1} \\ \boldsymbol{D}_{m_2} \end{pmatrix} = \boldsymbol{V_1}\boldsymbol{D}_{m_E}^*\boldsymbol{V_3} \tag{44}$$

$$\underline{\boldsymbol{B}^*} = \begin{pmatrix} \boldsymbol{B_1} \\ \boldsymbol{B_2} \end{pmatrix} = \boldsymbol{V_1}\boldsymbol{B}_E^*\boldsymbol{V_4}, \tag{45}$$

where $\boldsymbol{V_1}$ through $\boldsymbol{V_4}$ are the conversion matrices determined by a HEN structure and bypass locations. Their derivations are discussed in the succeeding section. With these reorganizations, an equivalent model to Eq. 32 is

$$\begin{pmatrix} \boldsymbol{\delta \underline{T}}^t \\ \boldsymbol{\delta \underline{T}}^m \end{pmatrix} = \begin{pmatrix} \boldsymbol{B_1} \\ \boldsymbol{B_2} \end{pmatrix}\boldsymbol{\delta \underline{f}} + \begin{pmatrix} \boldsymbol{D}_{t_{11}} & \boldsymbol{D}_{t_{12}} \\ \boldsymbol{D}_{t_{21}} & \boldsymbol{D}_{t_{22}} \end{pmatrix}\begin{pmatrix} \boldsymbol{\delta \underline{T}}^s \\ \boldsymbol{\delta \underline{T}}^m \end{pmatrix} + \begin{pmatrix} \boldsymbol{D}_{m_1} \\ \boldsymbol{D}_{m_2} \end{pmatrix}\boldsymbol{\delta \underline{Mc}_P}. \tag{46}$$

The preceding model contains two equations:

$$\boldsymbol{\delta \underline{T}}^t = \boldsymbol{B_1}\boldsymbol{\delta \underline{f}} + \boldsymbol{D}_{t_{11}}\boldsymbol{\delta \underline{T}}^s + \boldsymbol{D}_{t_{12}}\boldsymbol{\delta \underline{T}}^m + \boldsymbol{D}_{m_1}\boldsymbol{\delta \underline{Mc}_P} \tag{47}$$

and

$$\boldsymbol{\delta \underline{T}}^m = \boldsymbol{B_2}\boldsymbol{\delta \underline{f}} + \boldsymbol{D}_{t_{21}}\boldsymbol{\delta \underline{T}}^s + \boldsymbol{D}_{t_{22}}\boldsymbol{\delta \underline{T}}^m + \boldsymbol{D}_{m_2}\boldsymbol{\delta \underline{Mc}_P}. \tag{48}$$

Equivalently, Eq. 48 can be written as

$$\boldsymbol{\delta \underline{T}}^m = \left(\boldsymbol{I} - \boldsymbol{D}_{t_{22}}\right)^{-1}\boldsymbol{B_2}\boldsymbol{\delta \underline{f}} + \left(\boldsymbol{I} - \boldsymbol{D}_{t_{22}}\right)^{-1}\boldsymbol{D}_{t_{21}}\boldsymbol{\delta \underline{T}}^s + \left(\boldsymbol{I} - \boldsymbol{D}_{t_{22}}\right)^{-1}\boldsymbol{D}_{m_2}\boldsymbol{\delta \underline{Mc}_p}. \tag{49}$$

Substituting Eq. 49 into Eq. 47 yields the following system DP&C model:

$$\boldsymbol{\delta \underline{T}}^t = \underline{\boldsymbol{B}}\boldsymbol{\delta \underline{f}} + \underline{\boldsymbol{D}_t}\boldsymbol{\delta \underline{T}}^s + \underline{\boldsymbol{D}_m}\boldsymbol{\delta \underline{Mc}_p}, \tag{50}$$

where

$$\underline{\boldsymbol{B}} = \boldsymbol{B}_1 + \boldsymbol{D}_{t_{12}}\left(\boldsymbol{I} - \boldsymbol{D}_{t_{22}}\right)^{-1}\boldsymbol{B}_2 \tag{51}$$

$$\underline{\boldsymbol{D}_t} = \boldsymbol{D}_{t_{11}} + \boldsymbol{D}_{t_{12}}\left(\boldsymbol{I} - \boldsymbol{D}_{t_{22}}\right)^{-1}\boldsymbol{D}_{t_{21}} = \left(\underline{\boldsymbol{D}_{t_h}}^T\ \underline{\boldsymbol{T}_{t_c}}^T\right)^T \tag{52}$$

$$\underline{\boldsymbol{D}_m} = \boldsymbol{D}_{m_1} + \boldsymbol{D}_{t_{12}}\left(\boldsymbol{I} - \boldsymbol{D}_{t_{22}}\right)^{-1}\boldsymbol{D}_{m_2} = \left(\underline{\boldsymbol{D}_{m_h}}^T\ \underline{\boldsymbol{D}_{m_c}}^T\right)^T. \tag{53}$$

In more detail, if the vectors of stream temperatures and heat-capacity flow rates are written based on the classification of stream types, the model in Eq. 50 can be written as

$$\begin{pmatrix}\boldsymbol{\delta}\underline{\boldsymbol{T}}_h^t\\ \boldsymbol{\delta}\underline{\boldsymbol{T}}_c^t\end{pmatrix} = \underline{\boldsymbol{B}}\,\boldsymbol{\delta}\underline{\boldsymbol{f}} + \left(\underline{\boldsymbol{D}_{t_h}}\ \underline{\boldsymbol{D}_{t_c}}\right)\begin{pmatrix}\boldsymbol{\delta}\underline{\boldsymbol{T}}_h^s\\ \boldsymbol{\delta}\underline{\boldsymbol{T}}_c^s\end{pmatrix} + \left(\underline{\boldsymbol{D}_{m_h}}\ \underline{\boldsymbol{D}_{m_c}}\right)\begin{pmatrix}\underline{\boldsymbol{\delta Mc_{P_h}}}\\ \underline{\boldsymbol{\delta Mc_{P_c}}}\end{pmatrix}, \tag{54}$$

where

$$\boldsymbol{\delta}\underline{\boldsymbol{T}}_h^t = \left(\delta T_{h_1}^t\ \delta T_{h_2}^t \cdots \delta T_{h_{N_h}}^t\right)^T \tag{55}$$

$$\boldsymbol{\delta}\underline{\boldsymbol{T}}_c^t = \left(\delta T_{c_1}^t\ \delta T_{c_2}^t \cdots \delta T_{c_{N_c}}^t\right)^T \tag{56}$$

$$\boldsymbol{\delta}\underline{\boldsymbol{f}} = \left(\left(\delta f_{E_1}\right)^T\ \left(\delta f_{E_2}\right)^T \cdots \left(\delta f_{E_{N_2}}\right)^T\right)^T \tag{57}$$

$$\boldsymbol{\delta}\underline{\boldsymbol{T}}_h^s = \left(\delta T_{h_1}^s\ \delta T_{h_2}^s \cdots \delta T_{h_{N_h}}^s\right)^T \tag{58}$$

$$\boldsymbol{\delta}\underline{\boldsymbol{T}}_c^s = \left(\delta T_{c_1}^s\ \delta T_{c_2}^s \cdots \delta T_{c_{N_c}}^s\right)^T \tag{59}$$

$$\underline{\boldsymbol{\delta Mc_{P_h}}} = \left(\delta Mc_{P_{h_1}}\ \delta Mc_{P_{h_2}} \cdots \delta Mc_{P_{h_{Nh}}}\right)^T \tag{60}$$

$$\underline{\boldsymbol{\delta Mc_{P_c}}} = \left(\delta Mc_{P_{c_1}}\ \delta Mc_{P_{c_2}} \cdots \delta Mc_{P_{c_{Nc}}}\right)^T. \tag{61}$$

Network Structural Representation

As stated in the preceding section, conversion matrices $\boldsymbol{V}_1$ through $\boldsymbol{V}_4$ in Eqs. 43 through 45 are structure dependent. To derive these matrices, we first define a structural matrix, namely $\boldsymbol{S}[(2N_e - N_{\text{split}}) \times 2N_e]$. Matrix $\boldsymbol{S}$ can be decomposed into two submatrices, $\boldsymbol{S}_1(N_s \times 2N_e)$ and $\boldsymbol{S}_2(N_m \times 2N_e)$. Their definitions are given below; a detailed example of constructing these matrices for a given HEN is presented in Appendix A.

Construction of $\boldsymbol{S}_1$. In submatrix $\boldsymbol{S}_1$, each row is designated for a hot or a cold stream. Note that a stream can be split into a number of branches, which enter different HEXs and then mix together. In this case, the splitting ratios are reflected in the elements of the row for that stream. The columns are divided into N_e pairs; each pair is assigned for a specific HEX. In each pair, the left column and the right column are, respectively, designated to a hot stream and a cold stream going through the HEX. Each element has a value between 0 and 1, where 0 represents the stream not going through the HEX; a fraction represents the splitting portion going through the HEX; and 1 means the stream going through the HEX with no splitting involved.

Construction of $\boldsymbol{S}_2$. In submatrix $\boldsymbol{S}_2$, each row is designated for the intermediate stream between two adjacent HEXs. The definition of columns is the same as that for submatrix $\boldsymbol{S}_1$. Each element of $\boldsymbol{S}_2$ represents one of the three connection modes of an intermediate stream with a HEX. We assign [1], {1}, or 0 to an element to represent an intermediate stream entering, leaving, or not going through a HEX, respectively.

Derivation of $\boldsymbol{V}_1$. Matrix $\boldsymbol{V}_1$ has the same dimension as matrix $\boldsymbol{S}$ $[(2N_e - N_{\text{split}}) \times 2N_e]$. Each column j in $\boldsymbol{V}_1$ is generated based on the same column in $\boldsymbol{S}$. If element $s_{k,j}$ $[N_s \le k \le (2N_e - N_{\text{split}})]$ is {1}, then let $v_{1_{k,j}}$ equal 1, and $v_{1_{i,j}}$ equal 0 $[1 \le i \le (2N_e - N_{\text{split}});\ i \ne k]$. If $s_{k,j}$ is [1], then let $v_{1_{k,j}}$ equal 0, and $v_{1_{i,j}}$ equal $s_{i,j}$ $[1 \le i \le (2N_e - N_{\text{split}});\ i \ne k]$. If the jth column in $\boldsymbol{S}$ does not contain {1} or [1], then let $v_{1_{i,j}}$ be $s_{i,j}$ $[1 \le i \le (2N_e - N_{\text{split}})]$.

Derivation of $\boldsymbol{V}_2$. Matrix $\boldsymbol{V}_2$ has the dimension of $[2N_e \times (2N_e - N_{\text{split}})]$. Each row in $\boldsymbol{V}_2$ is also obtained based on the corresponding column in $\boldsymbol{S}$.

If $s_{k,j}$ $[N_s \le k \le (2N_e - N_{\text{split}})]$ is {1}, then let $v_{2_{j,k}}$ be 0, and all the other elements in the jth row of v_2 can be either 1 or 0; $v_{2_{j,i}}$ can be 1 if $s_{i,j}$ is greater than 0, or be 0 if $s_{i,j}$ equals to 0 $(i \ne k)$.

If $s_{k,j}$ is [1], then let $v_{2_{j,k}}$ be 1, and $v_{2_{j,i}}$ be 0.

If the jth column in $\boldsymbol{S}$ does not contain {1} or [1], then let $v_{2_{j,i}}$ be 0 if $s_{i,j}$ equals to 0, or 1 if $s_{i,j}$ is greater than 0.

Derivation of $\boldsymbol{V}_3$. Matrix $\boldsymbol{V}_3$ has the dimension of $2N_e \times N_s$. If the jth of matrix $\boldsymbol{S}$ contains at most one of {1} and [1], then let $v_{3j,i}$ equal $s_{i,j}$ $(i = 1, 2, \cdots, N_s)$. If the jth column of $\boldsymbol{S}$ contains both {1} (in the lth row) and [1] (in the mth row), then the elements of the jth row of $\boldsymbol{V}_3$ can be determined in two ways. In the lth row, if $s_{l,k}$ is [1], and the kth column contains only one [1] and no {1}, or in the row, $s_{m,k}$ is {1} and the kth column contains only one {1} and no [1], then let $v_{3_{j,i}}$ equal $s_{i,k}$ $[1 \le i \le N_s;\ N_s \le k \le (2N_e - N_{\text{split}})]$.

Derivation of $\boldsymbol{V}_4$. Matrix $\boldsymbol{V}_4$ is determined by bypass selection in a HEN. Mathematically,

$$\boldsymbol{\delta}\underline{\boldsymbol{f}} = \boldsymbol{V}_4\,\boldsymbol{\delta}\underline{\boldsymbol{f}}', \tag{62}$$

where $\boldsymbol{\delta}\underline{\boldsymbol{f}}$ consists of all $2N_e$ bypass candidates of N_e HEXs; $\boldsymbol{\delta}\underline{\boldsymbol{f}}'$ has the bypasses selected from the $2N_e$ candidates.

Model-Based Optimal Bypass Selection

Utility units (that is, heaters and coolers) are commonly placed to heat or cool the streams just before leaving a HEN, although some industrial practices show that they can be placed in other locations. This has been widely used for effective control of stream target temperatures. The number of utility units is always much less than that of process streams in the network for the sake of energy savings. In addition to utility units, a bypass acts as a control mechanism for disturbance rejection (Linnhoff and Kotjabasakis, 1986; Calandranis and Stephanopoulos, 1988; Mathisen et al., 1991; Uzturk and Akman, 1997; Yan and Huang, 1998, 1999).

Another important assumption is the worst-case design. That is, the maximum positive and negative deviations of the HEN target temperatures occur at the extreme disturbance values of the supply temperatures and mass-capacity flow rates. This is, in fact, commonly adopted (such as Yee and Grossmann, 1990; Uzturk and Akman, 1997), although there are exceptions.

Theoretical basis

In the system DP&C model in Eq. 50, each bypass option is a potential manipulated variable. Note that splitting fraction ratios and multiple bypasses contribute degree of freedom, and can be used for control design (Calandranis and Stephanopoulos, 1988; Mathisen et al., 1991, 1992, 1994). These options are not considered here. However, the methodology can be used to deal with a network involving stream splitting. The number of bypass options in a network is always more than necessary. Thus, a bypass selection must be made in design. To do so, we can rewrite Eq. 50 in the following way:

$$\underline{\boldsymbol{B}}\,\underline{\delta \boldsymbol{f}} - \boldsymbol{d} = \boldsymbol{0}. \tag{63}$$

where

$$\boldsymbol{d} = \delta \underline{\boldsymbol{T}}^{t}_{\max} - \left(\underline{\boldsymbol{D}_t}\,\delta \underline{\boldsymbol{T}}^{s} + \underline{\boldsymbol{D}_m}\,\underline{\delta \boldsymbol{Mc}_P}\right). \tag{64}$$

Vectors $\delta \underline{\boldsymbol{T}}^{t}_{\max}$ $(N_s \times 1)$ contains the information of the maximum permissible deviations of stream target temperatures. These deviations can be positive and negative, which are designated by vectors $\delta \underline{\boldsymbol{T}}^{t(+)}_{\max}$ and $\delta \underline{\boldsymbol{T}}^{t(-)}_{\max}$, respectively. Vector $\boldsymbol{d}$ reflects the magnitude of control corrections needed to eliminated the influence of disturbances. Similarly, there will be vectors $\boldsymbol{d}^{(+)}$ and $\boldsymbol{d}^{(-)}$.

Substituting Eq. 62 into Eq. 63 yields

$$\underline{\boldsymbol{B}}\boldsymbol{V}_4\,\underline{\delta \boldsymbol{f}'} - \boldsymbol{d} = \boldsymbol{0}. \tag{65}$$

Practically, we can only perform the following optimization through selecting a subset of bypasses, $\underline{\delta \boldsymbol{f}'}$, and the nominal value of each bypass,

$$\min_{\underline{\delta \boldsymbol{f}'}} \| \boldsymbol{B}\boldsymbol{V}_4\,\underline{\delta \boldsymbol{f}'} - \boldsymbol{d} \|_2. \tag{66}$$

This is subject to the system model in Eq. 50.

In this task, two difficulties need be resolved. First, we need to know how to identify the inverse of nonsquared matrix $\boldsymbol{B}(N_s \times 2N_e)$. Second, we need to have a way to determine the values of the elements in $\underline{\delta \boldsymbol{f}'}$. Nobel and Daniel (1977) conducted an extensive study on the solution identification of similar mathematical problems. Two related theorems are adopted in this work (Appendix B), with necessary modifications in order to fit the scope of this work.

Bypass placement selection

The selected bypasses, $\underline{\delta \boldsymbol{f}'}$ $(N_{f'} \times 1)$, is a subset of $\underline{\delta \boldsymbol{f}}$, where

$$N_{f'} = N_s - N_u. \tag{67}$$

In design, we need to pair $N_{f'}$ bypasses with $N_{f'}$ streams whose output temperatures should be controlled, and where no heaters and/or coolers are involved. The pairing is based on the analysis of interactions between a set of manipulated variables (bypasses) and a set of controlled variables (target temperatures). RGA has been successfully used to measure system interaction and to identity the most favorable pairings of controlled variables and manipulated variables for a squared system (McAvoy, 1987). For the system in Eq. 50, however, the gain matrix, $\underline{\boldsymbol{B}}$, is nonsquared. Thus, the regular RGA cannot be used directly. Theorem 1 (Nobel and Daniel, 1977, Appendix B) can be used to identify the pseudoinverse $\underline{\boldsymbol{B}}^{+}$. The regular RGA is then extended to measure network interaction (Chang and Yu, 1992; Cao, 1996; Skogestad and Postlethwaite, 1996).

Let $\boldsymbol{R}$ be the transpose of the pseudoinverse of $\underline{\boldsymbol{B}}$ (that is, $\boldsymbol{R} = (\underline{\boldsymbol{B}}^{+})^{T}$). The extended RGA will be

$$\boldsymbol{\Lambda} = \underline{\boldsymbol{B}} \otimes \boldsymbol{R}. \tag{68}$$

The operator, $\otimes$, is defined the same as that in a regular RGA, that is,

$$\lambda_{i,j} = b_{i,j} r_{i,j} \qquad (i = 1, 2, \ldots, N_s;\ j = 1, 2, \ldots, 2N_e). \tag{69}$$

The basic pairing rule is the same as that in the regular RGA. That is, each controlled variable is paired to a manipulated variable such that the corresponding relative gain is positive and as close to 1 as possible. The implementation of this rule will lead to the generation of $\underline{\delta \boldsymbol{f}'}$ from $\delta \boldsymbol{f}$.

Disturbance rejection with minimum economic penalty

While a bypass of a HEX provides an opportunity to reject disturbances, its installation must cause an increment of heat-transfer area of the HEX, if the same heat load needs to be maintained. The capital cost is evaluated based on the traditional cost function (such as Yee and Grossmann, 1990).

A trade-off between the DR and cost must be made in the bypass selection process. Figure 2 illustrates qualitatively how the stream target temperature fluctuation (δT_i^t) and the increment of HEX area $(\Delta A_{E_j}/A_{E_j})$ are related to the nominal fraction of a bypass (f_{E_j}). The nominal fraction of a bypass, f_{E_j}, can be selected from 0 (equivalent to no bypass) to the upper limit, $f_{E_j}^{(\lim)}$ (to be discussed in the succeeding subsection). As shown in the figure, when f_{E_j} increases, δT_i^t decreases, but $\Delta A_{E_j}/A_{E_j}$ increases. If a complete rejection of disturbances at the steady state is preferred, then the optimal nominal fraction of the bypass should be $f_{E_j}^{\mathrm{opt}}$. Note that any nominal fraction below this value will not realize complete DR, although the HEX area increment is smaller. If any selection is beyond this value, the HEX area increment will be more, while the DR is at the same level. Certainly, this is not desirable.

Iterative design procedure

Based on the DP&C model and methodology just described, a design procedure is developed below to determine the optimal locations and nominal fractions of bypasses for a HEN.

Step 1. For a given HEN with all design data and disturbance information, form the following vectors for all streams: (1) $\boldsymbol{T}^s$, $\boldsymbol{T}^t$, and $\boldsymbol{Mc}_P$; (2) $\delta \underline{\boldsymbol{T}}^{s(+)}$, $\delta \underline{\boldsymbol{T}}^{s(-)}$, $\delta \boldsymbol{Mc}_P^{(+)}$, and $\delta \boldsymbol{Mc}_P^{(-)}$; and (3) $\delta \boldsymbol{T}^{t(+)}_{\max}$ and $\delta \boldsymbol{T}^{t(-)}_{\max}$.

Step 2. Construct structural matrix $\boldsymbol{S}$ and then derive conversion matrices $\boldsymbol{V}_1$ through $\boldsymbol{V}_3$ based on $\boldsymbol{S}$.

Step 3. Form bypass candidate vector $\delta \boldsymbol{f}$ according to Eq. 57, set all initial bypass nominal fractions to zero, and let conversion matrix $\boldsymbol{V}_4$ be an identity. In addition, set elements

$\left(f_{h_{E_i}}\right)_{\mathrm{old}}$ and $\left(f_{c_{E_i}}\right)_{\mathrm{old}}$ $(i = 1, 2, \ldots, Ne)$ to zero.

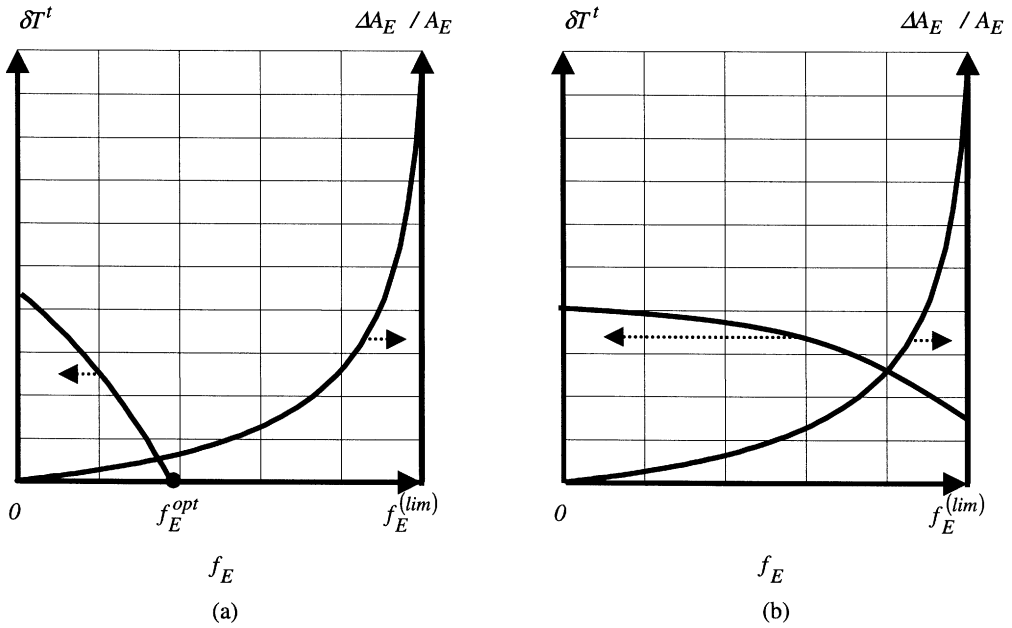

Figure 2. Qualitative relationship between a stream-target temperature fluctuation and a heat-transfer area change as a bypass fraction increases.

(a) Complete disturbance rejection when f_E is equal to or greater than f_E^{opt}; (b) Incomplete disturbance rejection with any bypass fraction.

Step 4. Construct the DP&C model for each HEX, according to Eq. 23. Note that the model coefficient matrices, $\boldsymbol{B}$, $\boldsymbol{D}_t$, and $\boldsymbol{D}_m$, depend on the nominal values of the bypasses in vector $\delta \boldsymbol{f}'$, which are updated in each iteration.

Step 5. Lump all the unit models to form a unit-based system DP&C model, as shown in Eq. 32.

Step 6. Convert the lumped system model to the system model in Eq. 50 or 54.

Step 7. Calculate the maximum positive and negative deviations of system target temperatures based on the known source disturbances as follows:

$$\underline{\boldsymbol{\delta T_d^t}}^{(+)} = \underline{\boldsymbol{D}}_{t_h} \underline{\boldsymbol{\delta T}}_h^{s(+)} + \underline{\boldsymbol{D}}_{t_c} \boldsymbol{\delta T}_c^{s(+)} + \underline{\boldsymbol{D}}_{m_h} \underline{\boldsymbol{\delta Mc}}_{P_h}^{(+)} - \underline{\boldsymbol{D}}_{m_c} \underline{\boldsymbol{\delta Mc}}_{P_c}^{(-)} \tag{70}$$

and

$$\underline{\boldsymbol{\delta T_d^t}}^{(-)} = \underline{\boldsymbol{D}}_{t_h} \underline{\boldsymbol{\delta T}}_h^{s(-)} + \underline{\boldsymbol{D}}_{t_c} \underline{\boldsymbol{\delta T}}_c^{s(-)} + \underline{\boldsymbol{D}}_{m_h} \underline{\boldsymbol{\delta Mc}}_{P_h}^{(-)} - \underline{\boldsymbol{D}}_{m_c} \underline{\boldsymbol{\delta Mc}}_{P_c}^{(+)} \tag{71}$$

where vectors $\underline{\boldsymbol{D}}_{t_h}$, $\underline{\boldsymbol{D}}_{t_c}$, $\underline{\boldsymbol{D}}_{m_h}$, and $\underline{\boldsymbol{D}}_{m_c}$ are defined in Eqs. 52 and 53.

Step 8. Compare vectors $\underline{\boldsymbol{\delta T_d^t}}^{(+)}$ and $\underline{\boldsymbol{\delta T_d^t}}^{(-)}$, on the element-by-element basis, with the maximum permissible target temperature vectors, $\underline{\boldsymbol{\delta T}}_{\max}^{t(+)}$ and $\underline{\boldsymbol{\delta T}}_{\max}^{t(-)}$, respectively, and then determine the necessary control correction vectors, $\boldsymbol{d}^{(+)}$ and $\boldsymbol{d}^{(-)}$, where

$$d_i^{(+)} = \begin{cases} 0, & \delta T_{d_i}^{t(+)} \le \delta T_{\max_i}^{t(+)}; \\ & i = 1, 2, \ldots, N_s \\ \delta T_{\max_i}^{t(+)} - \delta T_{d_i}^{t(+)}, & \text{otherwise} \end{cases} \tag{72}$$

$$d_i^{(-)} = \begin{cases} 0, & \delta T_{d_i}^{t(-)} \ge \delta T_{\max_i}^{t(-)}; \\ & i = 1, 2, \ldots, N_s. \\ \delta T_{\max_i}^{t(-)} - \delta T_{d_i}^{t(-)}, & \text{otherwise} \end{cases} \tag{73}$$

Step 9. Calculate the extended RGA, according to Eq. 68.

Step 10. Identify a subset of manipulated variables in $\boldsymbol{\delta f}$, pair each element in this vector with a controlled variable in $\underline{\boldsymbol{\delta T}}^t$ according to the paring rules in the section titled "Bypass Placement." The pairing generates $\underline{\boldsymbol{\delta f}}'$, where only preferred bypasses are included. Then derive conversion matrix $\boldsymbol{V}_4$ through checking the locations of the selected elements in the extended RGA, $\boldsymbol{\Lambda}$. If $\lambda_{i,j}$ is selected, then $\boldsymbol{v}_{4_{j,i}}$ is set to 1; otherwise, $v_{4_{j,i}}$ is set to zero.

Step 11. Calculate the nominal fraction of each bypass in $\underline{\boldsymbol{\delta f}}'$, based on $\boldsymbol{d}^{(+)}$ and $\boldsymbol{d}^{(-)}$ derived in Step 8. Here $\underline{\boldsymbol{\delta f}}'^{(+)}$ and $\underline{\boldsymbol{\delta f}}'_{(-)}$ are calculated using Theorem 2 in Appendix B.

Step 12. For each selected bypass, check to see if its fraction violates the upper permissible value in the following way:

$$|\delta f'^{(+)}_{h_{E_i}}| + |\delta f'^{(-)}_{h_{E_i}}| \le f^{(\lim)}_{h_{E_i}};$$

if the hot-stream-side bypass is placed on E_i, (74)

or

$$|\delta f'^{(+)}_{c_{E_i}}| + |\delta f'^{(-)}_{c_{E_i}}| \le f^{(\lim)}_{c_{E_i}};$$

if the cold-stream-side bypass is placed on E_i, (75)

where

$$f^{(\lim)}_{h_{E_i}} = \frac{T^t_{h_{E_i}} - T^s_{c_{E_i}} - \Delta T_{\min}}{T^s_{h_{E_i}} - T^s_{c_{E_i}} - \Delta T_{\min}} \tag{76}$$

$$f_{c_{E_i}}^{(\lim)} = \frac{T_{h_{E_i}}^{s} - T_{c_{E_i}}^{t} - \Delta T_{\min}}{T_{h_{E_i}}^{s} - T_{c_{E_i}}^{s} - \Delta T_{\min}}. \quad (77)$$

The two preceding equations are derived based on the requirement of minimum-temperature driving force for each HEX; Appendix C gives the details.

If the criteria in Eqs. 74 and 75 hold for each HEX, go on to the next step. Otherwise, stop the iteration. In this case, the resultant design is not satisfactory, since a complete rejection of disturbances cannot be realized. The process designer needs to make a decision on the acceptance of the design based on the calculated output deviations of stream temperatures.

If some inequality constrains are not satisfied for some selected bypasses, this indicates that the HEN system cannot reject completely the disturbances under the target temperature constraints. A trade-off should be then made to either relax relevant target temperature constraints or permit partial disturbance rejection.

Step 13. Update the nominal value of each selected bypass based on the following formulas:

$$\left(f_{h_{E_i}}\right)_{\text{new}} = -\min\left\{\delta f_{h_{E_i}}^{\prime(+)},\ \delta f_{h_{E_i}}^{\prime(-)}\right\}$$

if the hot-stream-side bypass is placed on E_i, (78)

or

$$\left(f_{c_{E_i}}\right)_{\text{new}} = -\min\left\{\delta f_{c_{E_i}}^{\prime(+)},\ \delta f_{c_{E_i}}^{\prime(-)}\right\}$$

if the cold-stream-side bypass is placed on E_i. (79)

Step 14. Check whether or not the iteration process should be terminated using the following criteria:

$$\left|\left(f_{h_{E_i}}\right)_{\text{new}} - \left(f_{h_{E_i}}\right)_{\text{old}}\right| \le \epsilon \quad (80)$$

and

$$\left|\left(f_{c_{E_i}}\right)_{\text{new}} - \left(f_{c_{E_i}}\right)_{\text{old}}\right| \le \epsilon, \quad (81)$$

where $(f_{h_{E_i}})_{\text{old}}$ and/or $(f_{c_{E_i}})_{\text{old}}$ are the bypass nominal fractions of exchanger E_i calculated in the preceding iteration; constant ϵ is a small nonnegative number representing a permissible computational error. Alternatively, the stopping criterion can also be counted in the relative change of the bypass nominal fractions. Note that every selected bypass should pass this checking. If any one of them fails, then let $(f_{h_{E_i}})_{\text{old}}$ equal $(f_{h_{E_i}})_{\text{new}}$ and $(f_{c_{E_i}})_{\text{old}}$ equal $(f_{c_{E_i}})_{\text{new}}$, and keep all other nominal fractions of those not selected bypasses at zero, and let conversion matrix $\boldsymbol{V}_4$ be an identity. After this, go to Step 4 for a new iteration; otherwise, go to the next step.

Step 15. Develop the final HEN retrofit design with the selected bypasses. Meanwhile, estimate the cost increment for each HEX where a bypass is placed. In addition, use the system model to calculate stream output deviations.

Note that in running the design procedure, matrices $\boldsymbol{B}$, $\boldsymbol{D}_t$, and $\boldsymbol{D}_m$ are all updated in each iteration. This is essentially a piecewise linearization approach that greatly reduces any significant errors caused by one-step linearization. Therefore, the final solution is always excellent, if not optimal. In this work, the optimal solution is defined as the one realizing complete disturbance rejection at the steady state, while the increment of heat-transfer areas of HEXs reaches the minimum. It should be pointed out that a global solution cannot be guaranteed.

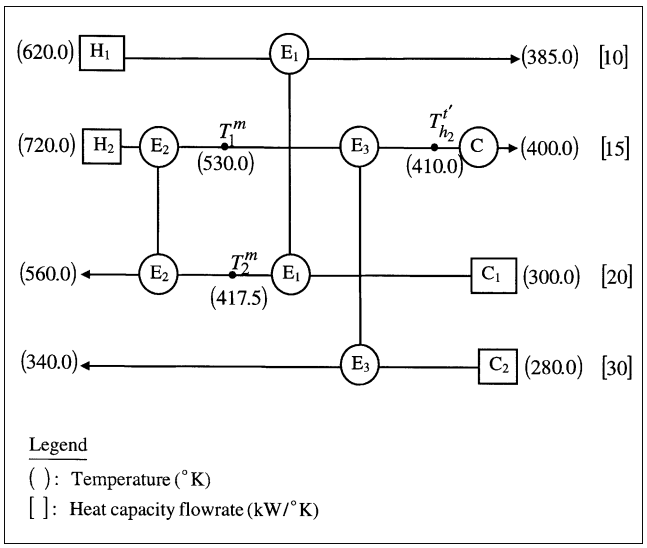

Figure 3. Four-stream HEN (Yee and Grossmann, 1990).

Case Studies

In this section, three HEN bypass design synthesis problems are studied. The resultant HENs are compared with known solutions in terms of DR and cost.

Case 1: Design of bypasses and control loops for a four-stream HEN

A HEN problem is shown in Figure 3, which was studied by Yee and Grossmann (1990). Table 1 lists the steady-state design data as well as disturbance information and control requirements.

Solution Derivation. The main steps in implementing the design procedure in the proceeding section are delineated below. The structural matrix, $\boldsymbol{S}$, derived in Step 2 is

$$\boldsymbol{S} = \begin{pmatrix} 1 & 0 & 0 & 0 & 0 & 0 \\ 0 & 0 & 1 & 0 & 1 & 0 \\ 0 & 1 & 0 & 1 & 0 & 1 \\ 0 & 0 & 0 & 0 & 0 & 0 \\ 0 & 0 & \{1\} & 0 & [1] & 0 \\ 0 & \{1\} & 0 & [1] & 0 & 0 \end{pmatrix} \quad (82)$$

Table 1. Design Data for the Four-Stream HEN Synthesis Problem

Stream No.	T^s (K)	T^t (K)	Mc_P (kW/K)	$\delta T^{s(+)}$ (K)	$\delta T^{s(-)}$ (K)	$\delta T_{\max}^{t(+)}$ (K)	$\delta T_{\max}^{t(-)}$ (K)
H_1	620.0	385.0	10.0	5	0	0	0
H_2	720.0	400.0	15.0	0	0	5.5	−5.5
C_1	300.0	560.0	20.0	0	−5	0	0
C_2	280.0	340.0	30.0	0	−5	4.0	−4.0

For clarity, Table 2 provides the detail definitions of the rows and columns of the matrix. According this matrix, conversion matrices V_1 through V_3 are obtained below:

$$V_1 = \begin{pmatrix} 1 & 0 & 0 & 0 & 0 & 0 \\ 0 & 0 & 0 & 0 & 1 & 0 \\ 0 & 0 & 0 & 1 & 0 & 0 \\ 0 & 0 & 0 & 0 & 0 & 1 \\ 0 & 0 & 1 & 0 & 0 & 0 \\ 0 & 1 & 0 & 0 & 0 & 0 \end{pmatrix} \tag{83}$$

$$V_2 = \begin{pmatrix} 1 & 0 & 0 & 0 & 0 & 0 \\ 0 & 0 & 1 & 0 & 0 & 0 \\ 0 & 1 & 0 & 0 & 0 & 0 \\ 0 & 0 & 0 & 0 & 0 & 1 \\ 0 & 0 & 0 & 0 & 1 & 0 \\ 0 & 0 & 0 & 1 & 0 & 0 \end{pmatrix} \tag{84}$$

$$V_3 = \begin{pmatrix} 1 & 0 & 0 & 0 \\ 0 & 0 & 1 & 0 \\ 0 & 1 & 0 & 0 \\ 0 & 0 & 1 & 0 \\ 0 & 1 & 0 & 0 \\ 0 & 0 & 0 & 1 \end{pmatrix}. \tag{85}$$

In Step 3, the bypass candidates for the three HEXs are identified below:

$$\delta \underline{f} = \left(\delta f_{h_{E_1}} \; \delta f_{c_{E_1}} \; \delta f_{h_{E_2}} \; \delta f_{c_{E_2}} \; \delta f_{h_{E_3}} \; \delta \underline{f}_{c_{E_3}} \right)^T. \tag{86}$$

At this stage, matrix V_4 (6×6) is an identity.

In Steps 4 and 5, the following unit-based system model can be obtained:

$$\begin{pmatrix} \delta T^t_{h_1} \\ \delta T^m_2 \\ \delta T^m_1 \\ \delta T^t_{c_1} \\ \delta T^t_{h_2} \\ \delta T^t_{c_2} \end{pmatrix} = \begin{pmatrix} 86.3 & 43.1 & 0 & 0 & 0 & 0 \\ -43.1 & -21.6 & 0 & 0 & 0 & 0 \\ 0 & 0 & 59.7 & 44.8 & 0 & 0 \\ 0 & 0 & -44.8 & -33.6 & 0 & 0 \\ 0 & 0 & 0 & 0 & 28.8 & 14.4 \\ 0 & 0 & 0 & 0 & -14.4 & -7.2 \end{pmatrix} \begin{pmatrix} \delta f_{h_{E_1}} \\ \delta f_{c_{E_1}} \\ \delta f_{h_{E_2}} \\ \delta f_{c_{E_2}} \\ \delta f_{h_{E_3}} \\ \delta f_{c_{E_3}} \end{pmatrix} + \begin{pmatrix} 0.266 & 0.734 & 0 & 0 & 0 & 0 \\ 0.367 & 0.633 & 0 & 0 & 0 & 0 \\ 0 & 0 & 0.372 & 0.628 & 0 & 0 \\ 0 & 0 & 0.471 & 0.529 & 0 & 0 \\ 0 & 0 & 0 & 0 & 0.52 & 0.48 \\ 0 & 0 & 0 & 0 & 0.24 & 0.76 \end{pmatrix}$$

$$\times \begin{pmatrix} \delta T^s_{h_1} \\ \delta T^s_{c_1} \\ \delta T^s_{h_2} \\ \delta T^m_2 \\ \delta T^m_1 \\ \delta T^s_{c_2} \end{pmatrix} + \begin{pmatrix} 14.9 & -2.16 & 0 & 0 & 0 & 0 \\ 4.31 & -4.80 & 0 & 0 & 0 & 0 \\ 0 & 0 & 8.69 & -2.24 & 0 & 0 \\ 0 & 0 & 2.98 & -5.45 & 0 & 0 \\ 0 & 0 & 0 & 0 & 6.08 & -0.48 \\ 0 & 0 & 0 & 0 & 0.96 & -1.76 \end{pmatrix} \begin{pmatrix} \delta Mc_{P_{h_1}} \\ \delta Mc_{P_{c_1}} \\ \delta Mc_{P_{h_2}} \\ \delta Mc_{P_{c_1}} \\ \delta Mc_{P_{h_2}} \\ \delta Mc_{P_{c_2}} \end{pmatrix} \tag{87}$$

After eliminating all intermediate temperatures in Step 6, the system model is

$$\begin{pmatrix} \delta T^t_{h_1} \\ \delta T^{t'}_{h_2} \\ \delta T^t_{c1} \\ \delta T^t_{c_2} \end{pmatrix} = \begin{pmatrix} 86.3 & 43.1 & 0 & 0 & 0 & 0 \\ -14.1 & -7.05 & 31.0 & 23.3 & 28.8 & 14.4 \\ -22.8 & -11.4 & -44.8 & -33.6 & 0 & 0 \\ -6.50 & -3.25 & 14.3 & 10.7 & -14.4 & -7.2 \end{pmatrix} \begin{pmatrix} \delta f_{h_{E_1}} \\ \delta f_{c_{E_1}} \\ \delta f_{h_{E_2}} \\ \delta f_{c_{E_2}} \\ \delta f_{h_{E_3}} \\ \delta f_{c_{E_3}} \end{pmatrix}$$

$$+ \begin{pmatrix} 0.266 & 0 & 0.734 & 0 \\ 0.12 & 0.193 & 0.207 & 0.48 \\ 0.194 & 0.471 & 0.335 & 0 \\ 0.055 & 0.089 & 0.095 & 0.76 \end{pmatrix} \begin{pmatrix} \delta T^s_{h_1} \\ \delta T^s_{h_2} \\ \delta T^s_{c_1} \\ \delta T^s_{c_2} \end{pmatrix} + \begin{pmatrix} 14.9 & 0 & -2.16 & 0 \\ 1.41 & 10.6 & -2.73 & -0.48 \\ 2.28 & 2.98 & -7.98 & 0 \\ 0.65 & 3.05 & -1.26 & -1.76 \end{pmatrix} \begin{pmatrix} \delta Mc_{P_{h_1}} \\ \delta Mc_{P_{h_2}} \\ \delta Mc_{P_{c_1}} \\ \delta Mc_{P_{c_2}} \end{pmatrix} \tag{88}$$

In Step 7, $\delta \underline{T}_d^{(+)}$ and $\delta \underline{T}_d^{(-)}$ can be calculated based on the system model and disturbance information listed in Table 1. They are

$$\delta \underline{T}_d^{(+)} = (1.33 \quad 0.600 \quad 0.971 \quad 0.277)^T \tag{89}$$

$$\delta \underline{T}_d^{(-)} = (-3.67 \quad -3.43 \quad -1.67 \quad -4.28)^T. \tag{90}$$

On the other hand, we can form the vectors, $\delta \underline{T}_{\max}^{(+)}$ and $\delta \underline{T}_{\max}^{(-)}$ from Table 1:

$$\delta \underline{T}_{\max}^{(+)} = (0 \quad 5.5 \quad 0 \quad 4.0)^T \tag{91}$$

$$\delta \underline{T}_{\max}^{(-)} = (0 \quad -5.5 \quad 0 \quad -4.0)^T. \tag{92}$$

Thus, in Step 8, we can obtain $\boldsymbol{d}^{(+)}$ and $\boldsymbol{d}^{(-)}$ according to Eqs. 72 and 73:

$$\boldsymbol{d}^{(+)} = (-1.33 \quad 0 \quad -0.97 \quad 0)^T \tag{93}$$

$$\boldsymbol{d}^{(-)} = (3.67 \quad 0 \quad 1.67 \quad 0.277)^T. \tag{94}$$

In Step 9 the pseudoinverse of matrix $\underline{\boldsymbol{B}}$ is calculated, and the extended RGA is obtained below, where the detailed steps are shown in Appendix D:

$$\boldsymbol{\Lambda} = \begin{pmatrix} 0.751 & 0.188 & 0 & 0 & 0 & 0 \\ 0.012 & 0.003 & 0.093 & 0.052 & 0.561 & 0.14 \\ 0.026 & 0.007 & 0.462 & 0.260 & 0 & 0 \\ 0.011 & 0.003 & 0.086 & 0.048 & 0.239 & 0.06 \end{pmatrix}. \tag{95}$$

In Step 10, the manipulated and controlled variables are paired as: (1) $T_{h_1}^t$ with $f_{h_{E_1}}$, (2) $T_{c_2}^t$ with $f_{h_{E_2}}$, (3) $T_{c_2}^t$ with $f_{h_{E_3}}$, and (4) $T_{h(2)}^{t'}$ with $f_{c_{E_3}}$, according to the paring rule.

Thus, the selected bypass vector is

$$\underline{\delta \boldsymbol{f}'} = \left(\delta f_{h_{E_1}} \; \delta f_{c_{E_2}} \; \delta f_{h_{E_2}} \; \delta f_{h_{E_3}} \right)^T. \tag{96}$$

Correspondingly,

$$\boldsymbol{V}_4 = \begin{pmatrix} 1 & 0 & 0 & 0 & 0 & 0 \\ 0 & 0 & 0 & 0 & 0 & 1 \\ 0 & 0 & 1 & 0 & 0 & 0 \\ 0 & 0 & 0 & 0 & 1 & 0 \end{pmatrix}^T. \tag{97}$$

Note that the paring, $T_{h_2}^{t'}$ with $f_{c_{E_3}}$, is related to the target temperature that is to be controlled by a utility unit. Hence, it is not to be considered further; we only discuss the other three pairs. The reduced output and control vectors are $\delta \underline{\boldsymbol{T}}_R^t = (\delta T_{h_1}^t \;\; \delta T_{c_1}^t \;\; \delta T_{c_2}^t)^T$ and $\underline{\delta \boldsymbol{f}'_R} = (\delta f_{h_1} \;\; \delta f_{h_2} \;\; \delta f_{h_3})^T$, respectively. Correspondingly, the reduced process gain matrix becomes

$$\underline{\boldsymbol{B}}_R = \begin{pmatrix} 86.3 & 0 & 0 \\ -22.8 & -44.8 & 0 \\ -6.50 & 14.3 & -14.4 \end{pmatrix}. \tag{98}$$

The required control corrections are

$$\boldsymbol{d}_R^{(+)} = (-1.33 \quad -0.97 \quad 0)^T \tag{99}$$

$$\boldsymbol{d}_R^{(-)} = (3.67 \quad 1.67 \quad 0.277)^T. \tag{100}$$

Hence, the required maneuverability of the bypasses is calculated in Step 11:

$$\underline{\delta \boldsymbol{f}'_R}^{(+)} = (-0.015 \quad 0.03 \quad 0.036)^T \tag{101}$$

$$\underline{\delta \boldsymbol{f}'_R}^{(-)} = (0.043 \quad -0.059 \quad -0.097)^T. \tag{102}$$

It is identified in Step 12 that the upper permissible values of the bypasses for $f_{h_{E_1}}^{(\lim)}$, $f_{h_{E_2}}^{(\lim)}$, and $f_{h_{E_3}}^{(\lim)}$ are 0.242, 0.35, and 0.5, respectively. In this first iterative procedure, Eq. 74 is satisfied for all three hot-stream side bypasses.

In Step 13, the new nominal fraction of each selected bypass is calculated using Eq. 78. They are 0.015, 0.059, and 0.097 for $(f_{h_{E_1}})_{\text{new}}$, $(f_{h_{E_2}})_{\text{new}}$, and $(f_{h_{E_3}})_{\text{new}}$, respectively. Note that $(f_{h_{E_i}})_{\text{old}}$ $(i = 1, 2, 3)$ are all equal to zero in the first iteration.

In Step 14, let the permissible computational error, ϵ, be 10^{-3}. It is found that the inequality in Eq. 80 doesn't hold.

Table 2. Structural Matrix Development

		Heat Exchanger						
		E_1		E_2		E_3		
Streams	Matrix $\boldsymbol{S}$	Hot Stream	Cold Stream	Hot Stream	Cold Stream	Hot Stream	Cold Stream	Streams
Process stream	H_1^{in}	1	0	0	0	0	0	H_1^{out}
	H_2^{in}	0	0	1	0	1	0	M_2
	C_1^{out}	0	1	0	1	0	1	C_1^{in}
	C_1^{out}	0	0	0	0	0	0	C_2^{in}
Intermediate stream	M_1	0	0	{1}	0	[1]	0	
		M_3	0	{1}	0	[1]	0	0

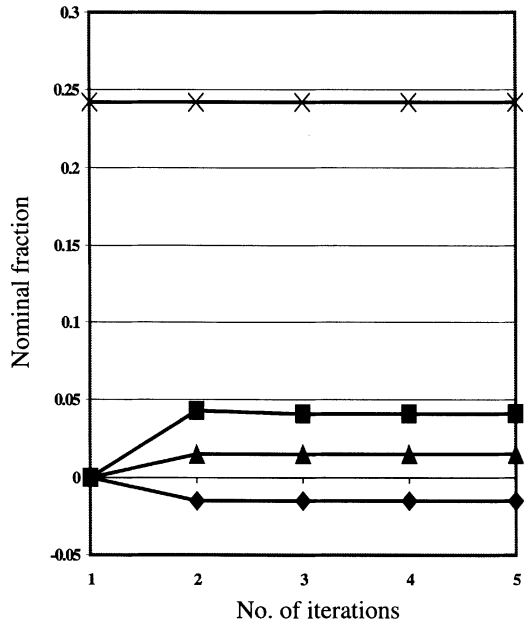

(a)

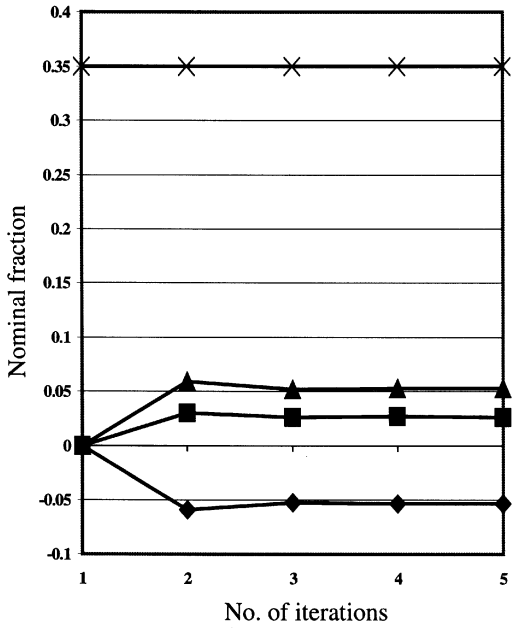

(b)

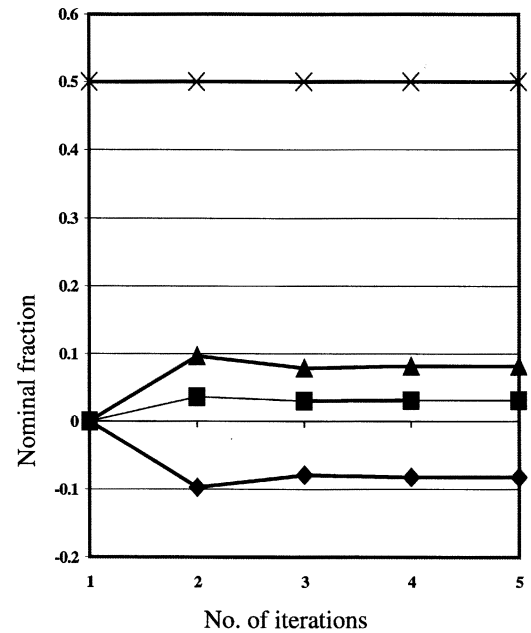

(c)

Figure 4. Determining bypass nominal fractions for the HEN experiencing only temperature disturbances (with initial bypass fractions of zero).

(a) Bypass selection for exchanger E_1; (b) bypass selection for exchanger E_2; (c) Bypass selection for exchanger E_3.

Legend : $\times$: $f_{h_{E_i}}^{(lim)}$ ■: $\delta f_{h_{E_i}}^{(+)}$ ◆: $\delta f_{h_{E_i}}^{(-)}$ ▲: $f_{h_{E_i}}$

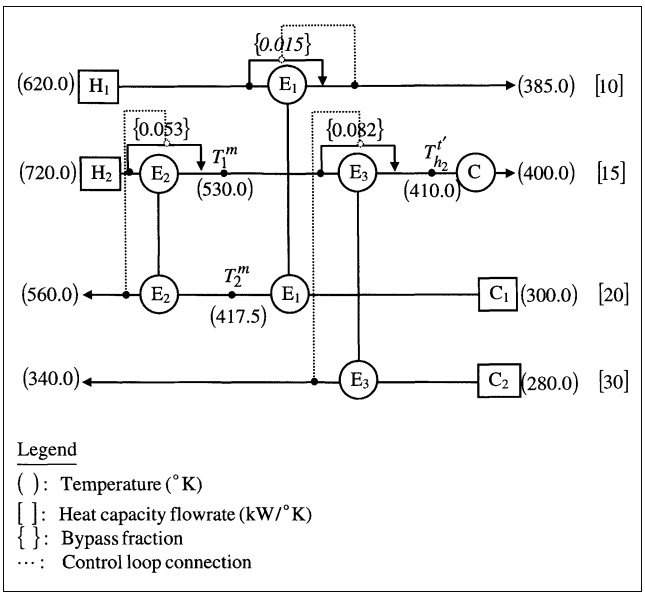

Figure 5. Optimal bypass design with control loops for the HEN by the DP&C approach.

Thus, let $(f_{h_{E_i}})_{\text{old}}$ equal $(f_{h_{E_i}})_{\text{new}}$ $(i = 1, 2, 3)$, and keep all other not selected bypass nominal fractions as zero, let conversion matrix $\boldsymbol{V}_4$ be an identity matrix, and then return to Step 4 for a new iteration. Figure 4 depicts the iterative selection processes for all three bypasses associated with exchangers E_1 and E_3. The finally selected bypass fractions are $f_{h_{E_1}}$, $f_{h_{E_2}}$, and $f_{h_{E_3}}$, with the nominal fractions of 0.015, 0.053, and 0.082, respectively.

In Step 15, three bypasses are placed in the network, as shown in Figure 5, where the related control schemes are also indicated. For this process, the system gain matrix, $\underline{\boldsymbol{B}}_R$, is

$$\underline{\boldsymbol{B}}_R = \begin{pmatrix} 88.9 & 0 & 0 \\ -2.35 & -49.9 & 0 \\ -6.70 & 15.9 & -17.1 \end{pmatrix}. \tag{103}$$

According to Eq. 68, the RGA for this case is

$$\boldsymbol{\Lambda} = \begin{pmatrix} 1 & 0 & 0 \\ 0 & 1 & 0 \\ 0 & 0 & 1 \end{pmatrix}. \tag{104}$$

Note that in this example four manipulated variables (three bypasses and one cooler flow rate) are selected to control the four stream target temperatures. This is inconsistent with the study on the degree of freedom. According to Calandranis and Stephanopoulos (1988), degree of freedom (N_{d_f}) for a HEN can be evaluated as

$$N_{d_f} = N_u + N_s + N_{b,\text{HEX}} + N_{\text{split}} - N_s^{cr}, \tag{105}$$

where N_u is the number of utility units; $N_{b,\text{HEX}}$ the total number of bypass candidates; N_{split} the total number of branches; and N_s^{cr} the number of streams across the pinch point. In our example,

$$N_{d_f} = 1 + 4 + 2 \times 3 + 0 - 0 = 11. \tag{106}$$

To demonstrate the superiority of the bypass placement, the relationships among the nominal fractions of bypasses, disturbance rejection quality, and economic penalty for all three HEXs used in the network are plotted in Figure 6. It is evident that the selected nominal fractions of bypasses are optimal, which realize the complete DR with the minimum economic penalty.

A further study shows that under the worst disturbances shown in Table 1, the stream target temperature fluctuations are

$$\boldsymbol{\delta}\underline{\boldsymbol{T}}^t = (0 \quad 4.04 \quad 0 \quad 3.50)^T. \tag{107}$$

Note that the design requirement listed in Table 1 is

$$\delta\underline{\boldsymbol{T}}_{\max}^{(\pm)} = (0 \quad \pm 5.5 \quad 0 \quad \pm 4.0)^T. \tag{108}$$

This shows that the design is very satisfactory. When the worst disturbances enter the network, the bypass fractions, $f_{h_{E_1}}$, $f_{h_{E_2}}$, and $f_{h_{E_3}}$, are adjusted to 0.007, 0.106, and 0.08, respectively.

Comparison. Uzturk and Akman (1997) studied the same problem. Table 3 provides the comparison of their bypass design (Figure 7) with ours (Figure 5). Our solution is 6% cheaper than that by Uzturk and Akman. This can be justified by examining the bypass nominal fractions (Table 4). Our design has much smaller values than Uzturk and Akman's. In addition, our design needs one control loop less than Uzturk and Akman's; this reduces the cost for the control system. More importantly, the RGA analysis reveals that our design has no system interaction among the three loops at the steady state. By contrast, the design in Figure 7 has considerable interactions among loops.

Discussion. It is very difficult to analyze quantitatively the rate of convergence in running the iterative design procedure. In solution identification, an initial bypass fraction (that is, initial point for search) for each bypass candidate equal to zero is preferred. This is physically more meaningful, as an initial HEN has no bypass on any HEX. It is suggested to try other starting points if the convergence is slow. In this example, however, the same bypass design can always be obtained for different initial points. For instance, initial bypass fractions of 0.5 are illustrated in Figure 8 to compare with the initial bypass fractions of 0 shown in Figure 4. After four iterations, the same optimal bypass fractions as those in Figure 4 are all obtained in Figure 8. Certainly, this does not mean true for all other cases.

A trade-off between DR and cost is always a concern in design. The design procedure provides complete profiles of DR and the increment of heat-transfer areas for a HEN, such as those in Figure 6. In this example, a complete DR with minimum economic penalty is preferred. Certainly, one can have different preference.

Further Study. The design just studied is under the temperature disturbances only. A more complicated situation is when the network experiences both temperature and heat-

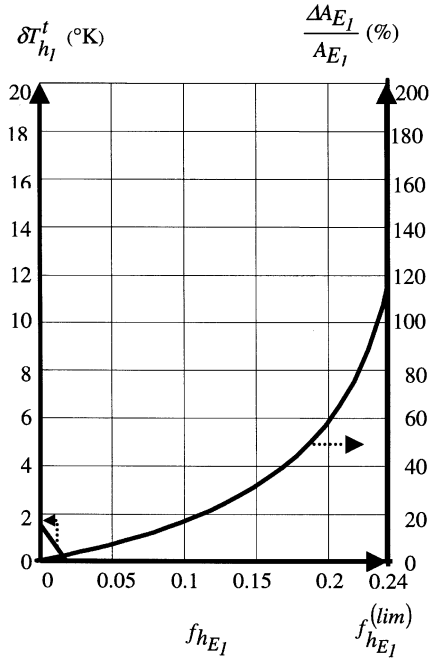

(a)

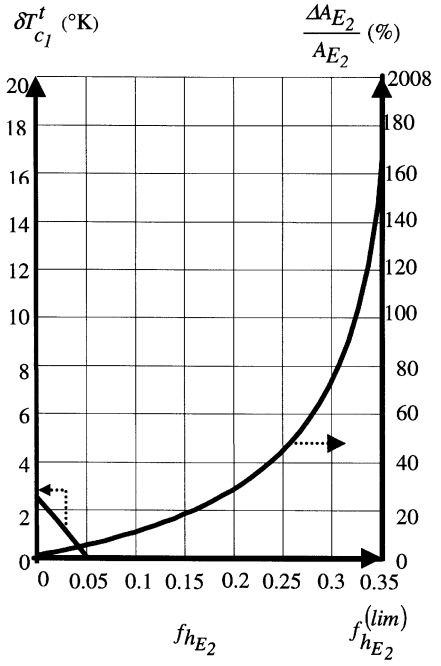

(b)

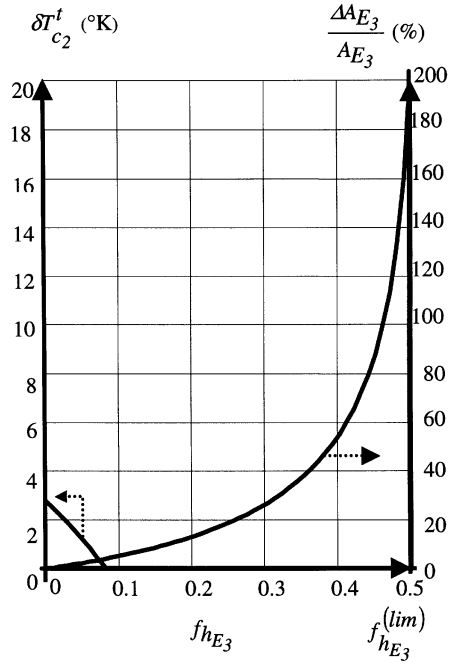

(c)

Figure 6. Change of the stream target temperatures and heat transfer areas as the function of the nominal fractions of bypasses of the three heat exchangers.

(a) Trade-off design for heat exchanger E_1; (b) trade-off design for heat exchanger E_2; (c) trade-off design for heat exchanger E_3.

capacity flow-rate disturbances. In this case, the temperature disturbances, $\delta \underline{T}^{s(+)}$ and $\delta \underline{T}^{s(-)}$, are the same as those listed in Table 1. The disturbances of heat-capacity flow rates are

$$\delta \underline{Mc_P}^{(+)} = (0.5 \quad 0 \quad 0 \quad 1.5)^T \tag{109}$$

$$\delta \underline{Mc_P}^{(-)} = (-0.5 \quad 0 \quad 0 \quad -1.5)^T. \tag{110}$$

With these disturbances, the bypass locations are the same as that in Figure 5. However, the nominal bypass fractions, $f_{h_{E_1}}$, $f_{h_{E_2}}$, and $f_{h_{E_3}}$, are equal to 0.082, 0.103, and 0.238, respec-

Table 3. Comparison of Heat-Transfer Areas of Different Designs

Heat Exchanger	Original Design (No Bypass), Area (m^2)	Our Design (with Bypass), Area (m^2)	Uzturk and Akman Design (with Bypass), Area (m^2)
E_1	34.7	35.4	39.1
E_2	42.3	44.3	49.2
E_3	22.8	23.7	25.8
ΣE_i	99.8	103.4	114.1
Cost	\$24 386	\$24 905	\$26 408

tively, after nine iterations of calculation (Figure 9). In this case, the total increment of heat transfer area is 12.5% for complete disturbance rejection. This is equivalent to 7.49% of cost increment.

Case 2: Improvement of a heat-integrated reaction-separation system

An industrial heat-integrated reaction separation system is depicted in Figure 10. A recycle stream from another process is heated from 98.9°C to 123.9°C and fed to column D_1. Feed A is preheated in a series of heat exchangers and then enters reactor R_1, where a slight endothermic reaction takes place. The product stream of reactor R_1 and the column overhead stream, after cooling, are mixed with feed B. This mixture stream is fed to reactor R_2 in which catalyst is very sensitive to its operating temperature; its performance will be seriously degraded if the temperature is unstable and above 110°C. This requires that the feed-stream temperature of reactor R_2 be strictly controlled between 96.1°C and 98.9°C. However, this process faces many disturbances including: (a) 10% of mass flow-rate change in the recycle stream; (b) 8.3% of mass flow-rate change in the column overhead stream; (c) column overhead temperature change from 132.2°C to 165.6°C; (d) feed A temperature change between 37.8°C and 65.6°C; and (e) feed B temperature change between 32.2°C and 48.9°C. These make the process inoperable, especially for reactor R_2. The process design data, source disturbances, and control requirements are listed in Table 5.

Yang et al. (1996) used the system DP model to modify a HEN associated with the process. Their solution is depicted in Figure 11, where all disturbance information is included. The location and nominal fraction of the bypass is heuristically placed to adjust the mass flow rate of the recycle stream going through exchanger E_1,

The design procedure developed in this work is used to identify the optimal bypass design. The system model is as follows:

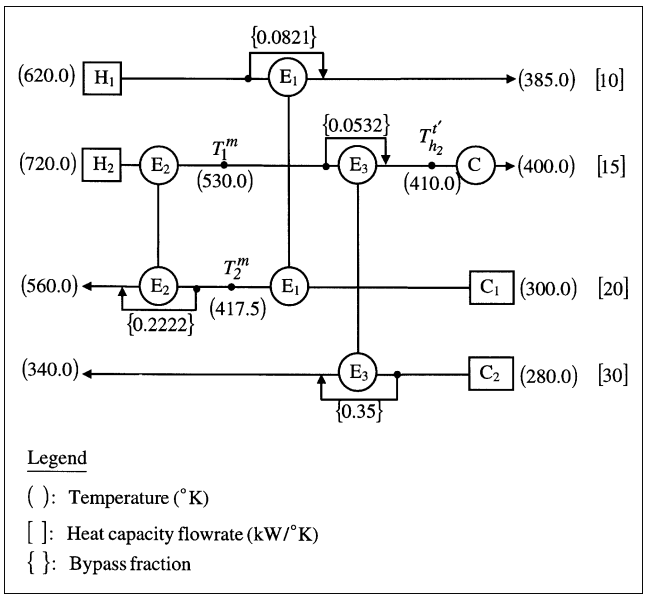

Figure 7. Bypass design for the same HEN (Uzturk and Arkam, 1997).

$$\begin{pmatrix} \delta T^t_{h_1} \\ \delta T^t_{h_2} \\ \delta T^t_{c_2} \\ \delta T^{t'}_{c_3} \end{pmatrix} = \begin{pmatrix} 10.9 & 7.5 & 0 & 0 \\ 0 & 0 & 40.9 & 46.7 \\ -9.1 & -6.25 & 0 & 0 \\ 0 & 0 & -46.7 & -53.3 \end{pmatrix} \begin{pmatrix} \delta f_{h_{E_1}} \\ \delta f_{c_{E_1}} \\ \delta f_{h_{E_2}} \\ \delta f_{c_{E_2}} \end{pmatrix} + \begin{pmatrix} 0.4 & 0 & 0.6 & 0 \\ 0 & 0.199 & 0 & 0.801 \\ 0.5 & 0 & 0.5 & 0 \\ 0 & 0.913 & 0 & 0.087 \end{pmatrix} \begin{pmatrix} \delta T^s_{h_1} \\ \delta T^s_{h_2} \\ \delta T^s_{c_2} \\ \delta T^s_{c_3} \end{pmatrix} + \begin{pmatrix} 0.774 & 0 & -0.23 & 0 \\ 0 & 3.38 & 0 & -2.95 \\ 0.304 & 0 & -0.576 & 0 \\ 0 & 2.58 & 0 & -3.4 \end{pmatrix} \begin{pmatrix} \delta Mc_{P_{h_1}} \\ \delta Mc_{P_{h_2}} \\ \delta Mc_{P_{c_2}} \\ \delta Mc_{P_{c_3}} \end{pmatrix}. \quad (111)$$

Table 4. Comparison of the System Interactions of Different Designs

	Our Design	Uzturk and Akman Design (1977)
Bypass fractions	$f_{h_{E_1}} = 0.015$; $f_{h_{E_2}} = 0.053$; $f_{h_{E_3}} = 0.082$	$f_{h_{E_1}} = 0.0821$; $f_{C_{E_2}} = 0.2222$; $f_{h_{E_3}} = 0.0532$; $f_{c_{E_3}} = 0.35$
No. of control loops	3	4
RGA analysis	$\text{RGA}(\underline{\boldsymbol{B}}_{\boldsymbol{R}}) = \begin{pmatrix} 1 & 0 & 0 \\ 0 & 1 & 0 \\ 0 & 0 & 1 \end{pmatrix}$	$\text{RGA}(\underline{\boldsymbol{B}}) = \begin{pmatrix} 0.938 & 0 & 0 & 0 \\ 0.015 & 0.33 & 0.145 & 0.371 \\ 0.033 & 0 & 0.721 & 0 \\ 0.014 & 0.14 & 0.134 & 0.158 \end{pmatrix}$

Note: Matrix $\underline{\boldsymbol{B}}$ is singular.

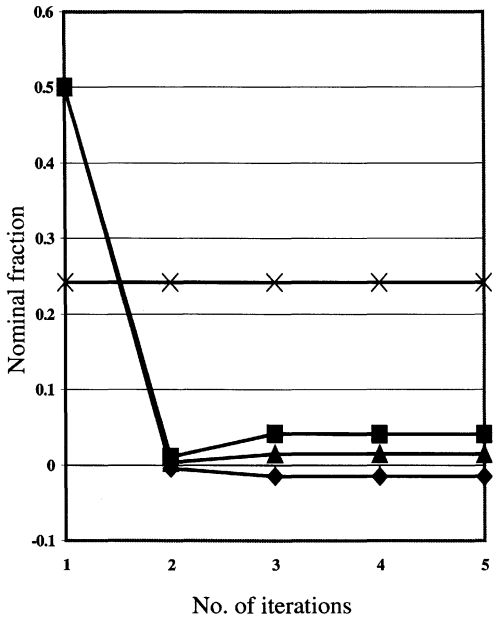

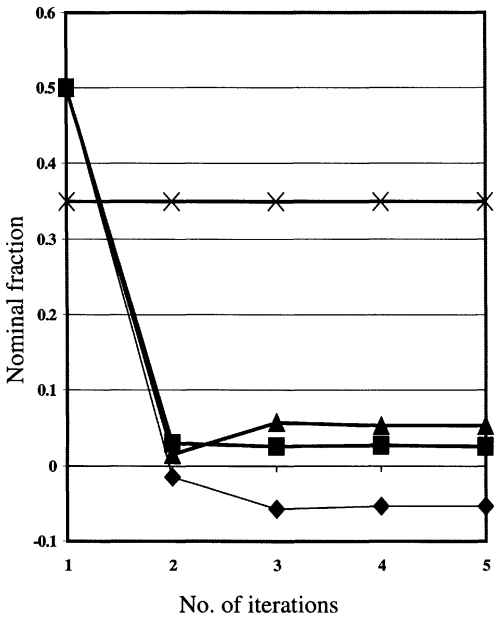

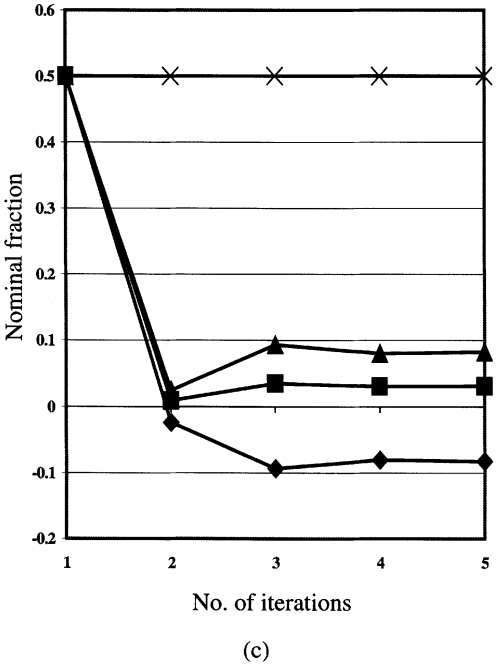

Figure 8. Determining bypass fractions for the HEN experiencing only temperature disturbances (with initial bypass fractions of 0.5).

(a) Bypass selection for heat exchanger E_1; (b) bypass selection for heat exchanger E_2; (c) bypass selection for heat exchanger E_3.

Legend : $\times$: $f_{h_{E_i}}^{(lim)}$ ■: $\delta f_{h_{E_i}}^{(+)}$ ◆: $\delta f_{h_{E_i}}^{(-)}$ ▲: $f_{h_{E_i}}$

Note that stream C_1 is not included in the model, since this stream mixed with streams H_1 and H_2 is not involved in heat exchange with any stream through a HEX. Its target temperature can be readily controlled by the heater placed at its end. Likewise, the target temperature of stream C_3 can be easily controlled by another heater (Figure 11). The remaining issue is how to reject disturbances for stream C_2 that experiences the disturbances from stream H_1 and itself. Based on the system model in Eq. 111, the RGA is obtained below:

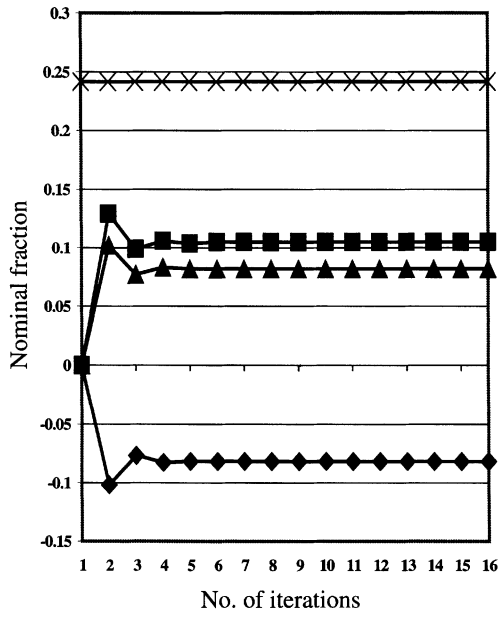

(a)

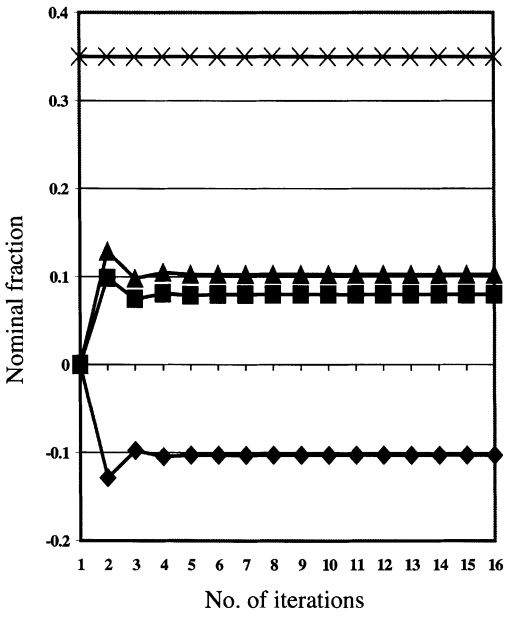

(b)

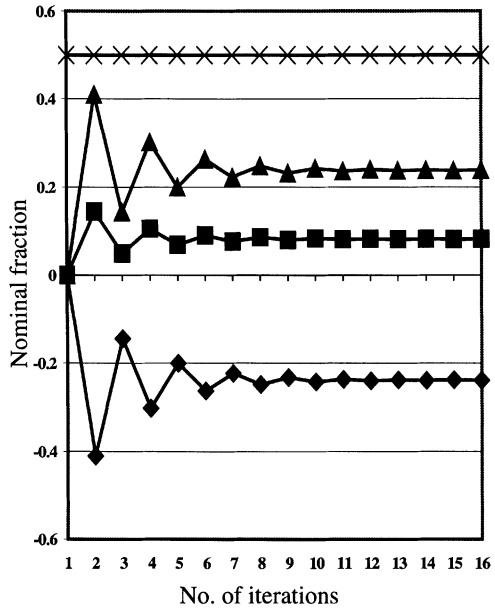

(c)

Figure 9. Determining bypass fractions for the HEN experiencing temperature disturbances and heat capacity flow-rate fluctuations (with initial bypass fractions of zero).

(a) Bypass selection for heat exchanger E_1; (b) bypass selection for heat exchanger E_2; (c) bypass selection for heat exchanger E_3.

Legend : $\times$: $f_{h_{E_i}}^{(lim)}$ ■: $\delta f_{h_{E_i}}^{(+)}$ ◆: $\delta f_{h_{E_i}}^{(-)}$ ▲: $f_{h_{E_i}}$

$$\mathbf{\Lambda} = \begin{pmatrix} 0.401 & 0.189 & 0 & 0 \\ 0 & 0 & 0.189 & 0.246 \\ 0.278 & 0.131 & 0 & 0 \\ 0 & 0 & 0.246 & 0.32 \end{pmatrix}. \qquad (112)$$

For stream C_2 to be controlled, we need to examine the elements in the third row of the RGA. The first element (0.278) in the row corresponds to the bypass on the hot-stream side of exchanger E_1, while the second one (0.131) is to the bypass on the cold-stream side of the same exchanger. Apparently, the placement of a bypass on the hot-stream side is a better choice than that on the cold-stream side of the example in controlling target temperature $\delta T_{c_2}^t$ by bypass $\delta f_{h_{E_1}}$

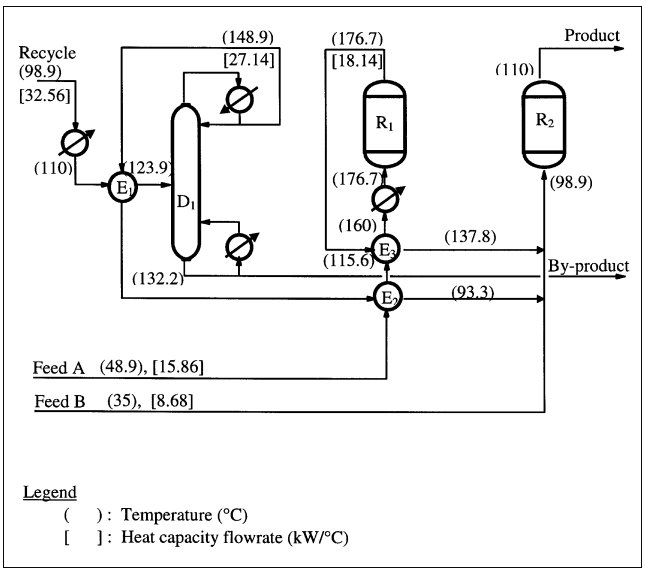

Figure 10. Heat-integrated reactor-separation process.

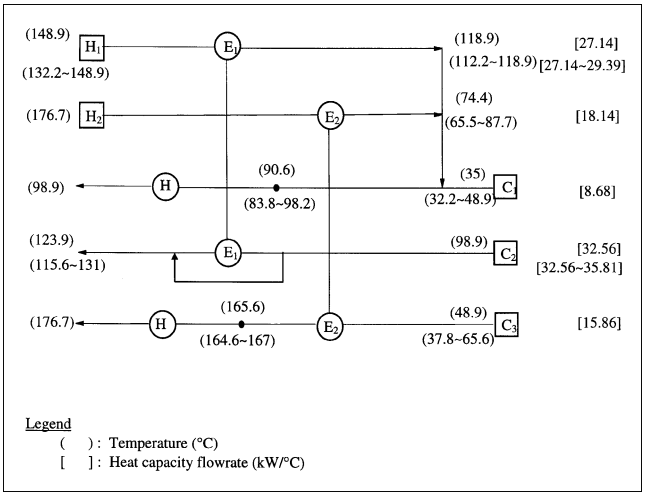

Figure 11. Modified HEN for the heat-integrated reactor-separation process (Yang et al., 1996).

(Yang et al., 1996). The nominal fraction of the bypass calculated by the design procedure is 0.092, which is below the upper limit (0.286). The process flowsheet with the new by-

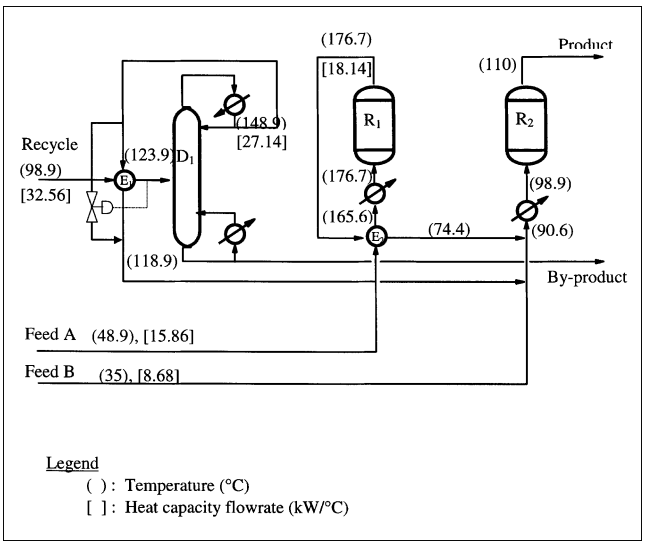

Figure 12. Heat-integrated reactor-separation process with the modified bypass and control loop by the DP&C approach.

pass is depicted in Figure 12. Due to the bypass placement, the heat-transfer area of exchanger E_1 is increased from 72.7 m^2 to 78.6 m^2 for complete DR. With these changes, the original operational problems are completely eliminated.

Case 3: Synthesis of a fairly complicated pinched HEN: 7SP4

The 7SP4 synthesis problem that has been extensively used with the assumption of constant temperatures and heat capacity flow rates is fairly complicated (Papotilias and Grossmann, 1983; Dolan et al., 1989). Huang and Fan (1994) imposed various disturbances and levels of control precision to it in order to study the controllability improvement through process synthesis. In this study, the solutions by Huang and Fan (1994) and Papotilias and Grossmann (1983) are selected for studying the bypass design and structural comparison. All pertinent design data of the problem are listed in Table 6. The pinch point of the network corresponds to 420°F assuring that the minimum tolerable temperature difference, ΔT_{min}, is 20°F.

Figure 13 depicts the network structure designed by Huang and Fan (1994) and the bypasses derived by the DP&C methodology. The system DP&C model is

Table 5. Design Data for the Heat-Integrated Reactor-Separator System Synthesis

Stream No.	T^s (°C)	T^t (°C)	Mc_P (kW/°C)	$\delta T^{s(+)}$ (°C)	$\delta T^{s(-)}$ (°C)	$\delta Mc_P^{(+)}$ (kW/°C)	$\delta Mc_P^{(-)}$ (kW/°C)	$\delta T_{max}^{t(+)}$ (°C)	$\delta T_{max}^{t(-)}$ (°C)
H_1	148.9	118.9	27.14	0	−16.7	2.25	0	0	−6.7
H_2	176.7	74.4	18.14	0	0	0	0	13.3	−8.9
C_1	35.0	98.9	8.68	13.9	−2.8	0	0	0	0
C_2	98.9	123.9	32.56	0	0	3.25	0	7.1	−8.3
C_3	48.9	176.7	15.86	16.7	−11.1	0	0	0	0

Table 6. Stream Data of Heat-Exchanger Network Synthesis Problem 7SP4

Stream No.	T^s (°F)	T^t (°F)	Mc_P (kBtu/h·°F)	$\delta T^{s(+)}$ (°F)	$\delta T^{s(-)}$ (°F)	$\delta Mc_P^{(+)}$ (kBtu/h·°F)	$\delta Mc_P^{(-)}$ (kBtu/h·°F)	$\delta T_{\max}^{t(+)}$ (°F)	$\delta T_{\max}^{t(-)}$ (°F)
H_1	675	150	15.0	3.0	4.0	1.0	0.5	1.5	−1.5
H_2	590	450	11.0	2.0	1.0	0.3	0.3	3.0	−3.0
H_3	540	115	4.5	6.0	8.0	0.1	0.1	2.0	−2.0
H_4	430	345	60.0	3.0	4.0	0.8	0.8	4.0	−4.0
H_5	400	100	12.0	3.0	5.0	0.1	0.1	1.0	−1.0
H_6	300	230	125.0	2.0	2.5	1.0	1.0	6.0	−6.0
C_1	60	710	47.0	3.0	6.0	1.2	1.2	4.0	−4.0

$$\begin{pmatrix} \delta T_{h_1}^{t'} \\ \delta T_{h_2}^{t} \\ \delta T_{h_3}^{t} \\ \delta T_{h_4}^{t} \\ \delta T_{h_6}^{t} \\ \delta T_{c_1}^{t'} \end{pmatrix} = \begin{pmatrix} 95.1 & 47.2 & 0 & 0 & 0 & 0 & -28.9 & -36.5 & 6.3 & 28 & -2.6 & -7.5 \\ 6.4 & 3.2 & 58.5 & 47.3 & 0 & 0 & -30.8 & -39 & -2.2 & -9.9 & -2.7 & -8 \\ 0 & 0 & 0 & 0 & 209.4 & 208.7 & 0 & 0 & 0 & 0 & 0 & 0 \\ 0 & 0 & 0 & 0 & 0 & 0 & 29.1 & 36.8 & 0 & 0 & -16.7 & -48.9 \\ 0 & 0 & 0 & 0 & 0 & 0 & 0 & 0 & 0 & 0 & 11 & 32.2 \\ -35.6 & -17.7 & -15 & -12.1 & -20 & -20 & -18.9 & -23.9 & -1.4 & -6.1 & -1.7 & -4.9 \end{pmatrix}$$

$$\times \begin{pmatrix} \delta_{H_{E_1}} \\ \delta f_{c_{E_1}} \\ \delta f_{h_{E_2}} \\ \delta f_{c_{E_2}} \\ \delta f_{h_{E_3}} \\ \delta f_{c_{E_3}} \\ \delta f_{h_{E_4}} \\ \delta f_{c_{E_4}} \\ \delta f_{h_{E_5}} \\ \delta f_{c_{E_5}} \\ \delta f_{h_{E_6}} \\ \delta f_{c_{E_6}} \end{pmatrix} + \begin{pmatrix} 0.06 & 0 & 0 & 0.57 & 0.07 & 0.22 \\ 0 & 0.22 & 0 & 0.6 & 0.07 & 0.01 \\ 0 & 0 & 0.11 & 0 & 0 & 0.89 \\ 0 & 0 & 0 & 0.43 & 0.44 & 0.04 \\ 0 & 0 & 0 & 0 & 0.71 & 0.29 \\ 0.33 & 0.2 & 0.08 & 0.37 & 0.04 & 0.01 \end{pmatrix} \begin{pmatrix} \delta T_{h_1}^{s} \\ \delta T_{h_2}^{s} \\ \delta T_{h_3}^{s} \\ \delta T_{h_4}^{s} \\ \delta T_{h_6}^{s} \\ \delta T_{c_1}^{s} \end{pmatrix} + \begin{pmatrix} 12.2 & 0 & 0 & 0.4 & 0 & -3.2 \\ 0.6 & 7.6 & 0 & 0.5 & 0 & -2.6 \\ 0 & 0 & 50.3 & 0 & 0 & -4.4 \\ 0 & 0 & 0 & 1 & 0.1 & -2 \\ 0 & 0 & 0 & 0 & 0.5 & -0.7 \\ 3 & 1.3 & 4.2 & 0.3 & 0 & -3.3 \end{pmatrix} \begin{pmatrix} \delta Mc_{P_{h_1}} \\ \delta Mc_{P_{h_2}} \\ \delta Mc_{P_{h_3}} \\ \delta Mc_{P_{h_4}} \\ \delta Mc_{P_{h_6}} \\ \delta Mc_{P_{c_1}} \end{pmatrix} \quad (113)$$

Note that stream H_5 is not included in the model, since this stream has no interaction with the rest of the network. Its target temperature can be readily controlled by the cooler placed at its end. Likewise, the target temperatures of stream H_1 and C_1 can be controlled by the utility units. What needs to be considered is to reject disturbances for streams H_1, H_5, and C_1. Based on the system DP&C model, the RGA is obtained below.

$$\Lambda = \begin{pmatrix} 0.547 & 0.134 & 0 & 0 & 0 & 0 & 0.08 & 0.129 & 0.003 & 0.067 & 0.002 & 0.021 \\ -0.007 & -0.002 & 0.482 & 0.315 & 0 & 0 & 0.063 & 0.101 & 0.001 & 0.02 & 0.002 & 0.017 \\ 0 & 0 & 0 & 0 & 0.501 & 0.498 & 0 & 0 & 0 & 0 & 0 & 0 \\ 0 & 0 & 0 & 0 & 0 & 0 & 0.092 & 0.147 & 0 & 0 & 0.058 & 0.495 \\ 0 & 0 & 0 & 0 & 0 & 0 & 0 & 0 & 0 & 0 & 0.038 & 0.323 \\ 0.213 & 0.052 & 0.107 & 0.07 & 0.001 & 0.001 & 0.149 & 0.238 & 0 & -0.001 & 0.005 & 0.039 \end{pmatrix}. \quad (114)$$

The upper limits for all the potential pass fractions are calculated using Eqs. 76 and 77:

$$f_{E_i}^{(\lim)} = (0 \quad 0.504 \quad 0.125 \quad 0.241 \quad 0.076 \quad 0 \quad 0.341 \quad 0 \quad 0.775 \quad 0 \quad 0.682 \quad 0). \quad (115)$$

For the DR of stream H_2, the second row of RGA needs to be examined. The element $\lambda_{2,3}$ (0.482) is greater than other elements. This corresponds to the bypass on the hot-stream

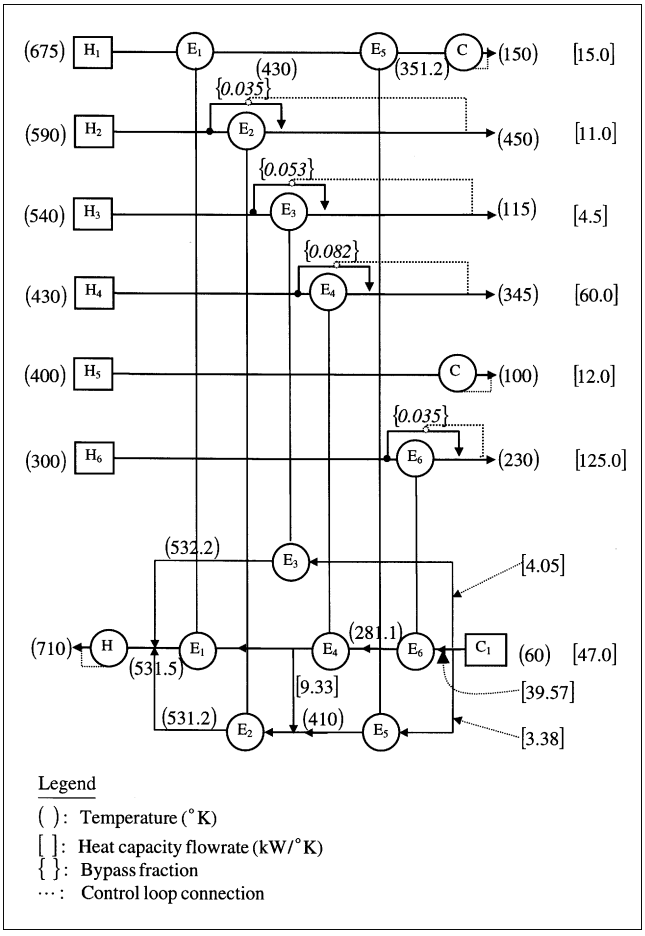

Figure 13. Solution A of the 7SP4 HEN synthesis problem (Huang and Fan, 1994) with the bypasses design by the DP&C approach.

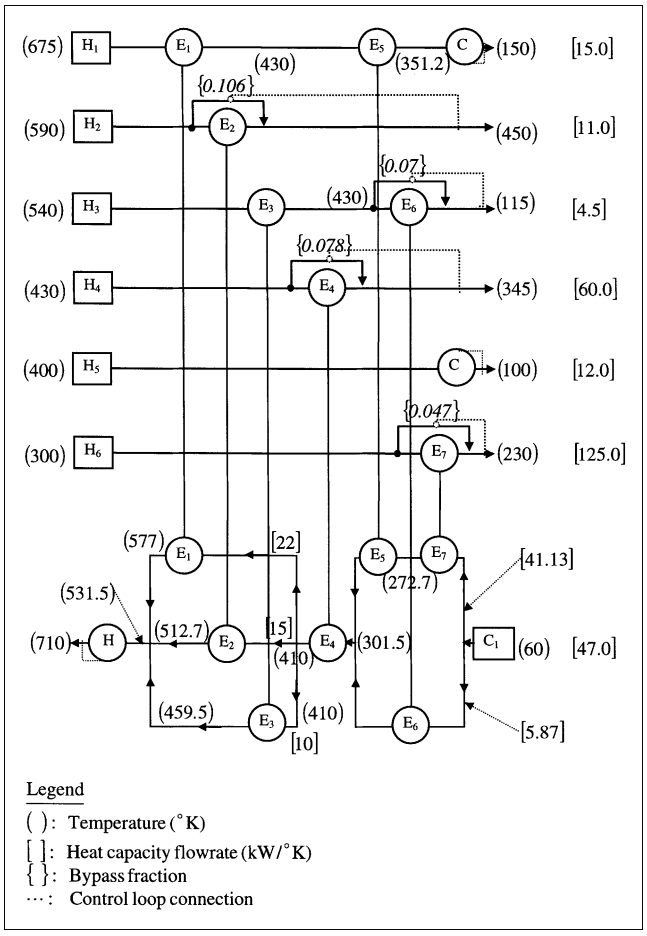

Figure 14. Solution B of the 7SP4 HEN synthesis problem (Papoulias and Grossmann, 1983) with the bypasses design by the DP&C approach.

side of exchanger E_2. For the same reason, after examining the third row of elements, the bypass on the hot-stream side of the exchanger E_3 is selected to control the target temperature of stream H_3. For stream H_4, the bypass on the cold-stream side of exchangers E_6 or E_4 should be selected, since $\lambda_{4,12}$ (0.495) and $\lambda_{4,8}$ (0.147) are closer to 1. They cannot be selected because $f_{E6,c}^{(\lim)}$ and $f_{E_{4,c}}^{(\lim)}$ equal 0. The next choice of bypass is on the hot-stream side of exchanger E_4. For the same reason, the bypass on the hot-stream side of exchanger E_6 needs to be selected to control the target temperature in stream H_6 (Figure 13).

For the network by Papotilias and Grossmarm (1983), the system DP&C model and the RGA can be derived in the same way. For simplicity, only the RGA is given below:

$$\mathbf{\Lambda} = \begin{pmatrix} 0.079 & 0.037 & 0 & 0 & 0 & 0 & 0 & 0 & 0.78 & 0.104 & 0 & 0 & 0 & 0 \\ 0 & 0 & 0.65 & 0.35 & 0 & 0 & 0 & 0 & 0 & 0 & 0 & 0 & 0 & 0 \\ 0 & 0 & 0 & 0 & 0.001 & 0 & 0 & 0 & 0 & 0 & 0.629 & 0.37 & 0 & 0 \\ 0 & 0 & 0 & 0 & 0 & 0 & 0.38 & 0.62 & 0 & 0 & 0 & 0 & 0 & 0 \\ 0 & 0 & 0 & 0 & 0 & 0 & 0 & 0 & 0 & 0 & 0 & 0 & 0.098 & 0.902 \\ 0.597 & 0.277 & 0 & 0 & 0.105 & 0.021 & 0 & 0 & 0 & 0 & 0 & 0 & 0 & 0 \end{pmatrix}. \quad (116)$$

The upper limits for the potential pass fractions are

$$f_{E_i}^{(\lim)} = (0 \quad 0.318 \quad 0.125 \quad 0.358 \quad 0 \quad 0.55 \quad 0.217 \quad 0 \quad 0.426 \quad 0.79 \quad 0.1 \quad 0.31 \quad 0.682 \quad 0.033) \quad (117)$$

A complete process flowsheet with bypasses is depicted in Figure 14.

The bypass design for the two HEN solutions are compared to each other. As summarized in Table 7, these two solutions all need four bypasses on four HEXs. The total cost for Solution A is 4.18% cheaper than that for solution B. However, the system interaction analysis based on λ-values shows that Solution B is somehow a little better than Solution A. A process designer can make a choice based on this information.

Table 7. Comparison of the Solutions for HEN Synthesis Problem 7SP4

Items	Solution A Huang and Fan (1994)	Solution B Papotilias and Grossmann (1983)
Bypass fractions	$f_{h_{E_2}} = 0.035$; $f_{h_{E_4}} = 0.082$; $f_{h_{E_3}} = 0.053$; $f_{h_{E_6}} = 0.035$	$f_{h_{E_2}} = 0.106$; $f_{h_{E_2}} = 0.07$; $f_{h_{E_4}} = 0.078$; $f_{h_{E_7}} = 0.047$
Areas of the HEXs before adding bypasses (m^2)	$A_1 = 29.32$; $A_4 = 67.48$; $A_2 = 15.78$; $A_5 = 5.84$; $A_3 = 39.57$; $A_6 = 63.6$	$A_1 = 37.44$; $A_4 = 84.33$; $A_2 = 13.6$; $A_5 = 25.36$; $A_3 = 5.7$; $A_6 = 8.19$; $A_7 = 56.08$
Areas of the HEXs after adding bypasses (m^2)	$A_2 = 16.81$; $A_4 = 72.71$; $A_3 = 56.65$; $A_6 = 64.24$	$A_2 = 17.07$; $A_6 = 10.30$; $A_4 = 93.24$; $A_7 = 56.82$
Total areas of all HEXs not including utility units, since they are the same. Solution A and B (m^2)	221.6	230.7
Total areas of all HEXs after adding bypasses (m^2)	245.6	245.9
Cost of the HEXs before adding bypasses (not including utility units)	\$49 393	\$52 419
Cost of the HEXs after adding bypasses (not including utility units)	\$52 424	\$54 617
Interaction analysis	$\lambda_{2,3} = 0.482$; $\lambda_{4,7} = 0.092$; $\lambda_{3,5} = 0.501$; $\lambda_{5,11} = 0.038$	$\lambda_{2,3} = 0.65$; $\lambda_{4,7} = 0.38$; $\lambda_{3,11} = 0.629$; $\lambda_{5,13} = 0.098$

Conclusion

Design of a cost-effective and high controllable heat-exchanger network (HEN) has both economical and operational significance. The major difficulty involved is how to choose the fewest bypasses and to determine their nominal fractions for complete disturbance rejection with minimum economic penalty. In this article, a unique system disturbance propagation and control (DP&C) model is developed to quantify disturbance propagation throughout a HEN and disturbance rejection by choosing bypasses. A model-based design procedure is also introduced for the development of a HEN with optimal bypass determination. The applications demonstrate its robustness and effectiveness. The modeling and design principles embedded in the methodology are general. They can be extended to the design of an optimal mass exchanger network with recycles for maximum disturbance rejection in a cost-effective way.

Acknowledgment

Financial support from the National Science Foundation (CTS-9414494) is gratefully acknowledged.

Notation

A = heat-transfer area
$\boldsymbol{B}$ = process-gain matrix
$\boldsymbol{d}$ = control-correction vector
$\boldsymbol{D_m}$ = heat-capacity flow-rate related disturbance-propagation matrix
$\boldsymbol{D_t}$ = temperature-related disturbance-propagation matrix
E = heat exchanger
f = bypass nominal fraction
δf = maximum fluctuation of bypass nominal fraction
$\boldsymbol{\delta f}$ = vector of maximum fluctuations of bypass nominal fractions
$\boldsymbol{I}$ = unit matrix
Mc_P = heat-capacity flow rate
δMc_P = maximum disturbance of heat-capacity flow rates
$\boldsymbol{\delta Mc_P}$ = vector of maximum disturbances of heat-capacity flow rates
N = number of streams, heat exchangers, or utilities
Q = heat duty of a heat exchanger
$\boldsymbol{R}$ = transpose of inversion of a process-gain matrix
$\boldsymbol{S}$ = structural matrix of a heat-exchanger network
T = temperature
δT = maximum temperature deviation of a stream
$\boldsymbol{\delta T}$ = vector of maximum temperature deviations of streams
ΔT = temperature difference
U = overall heat-transfer coefficient
$\boldsymbol{U}$ = matrix obtained from singular-value decomposition
$\boldsymbol{V}$ = matrix obtained from singular-value decomposition
$\boldsymbol{V_1}$ = conversion matrix related to output temperatures
$\boldsymbol{V_2}$ = conversion matrix related to input temperatures
$\boldsymbol{V_3}$ = conversion matrix related to input heat-capacity flow rates
$\boldsymbol{V_4}$ = conversion matrix related to bypass selections

Greek letters

ϵ = permissible computational error
$\boldsymbol{\Sigma}$ = matrix obtained from singular-value decomposition
$\boldsymbol{\Lambda}$ = relative gain array

Superscripts and subscripts

b = bypass
e = heat exchanger
i = input to a heat exchanger
in = input vector to a heat exchanger in a HEN
m = intermediate stream
o = output from a heat exchanger
out = output vector from a heat exchanger in a HEN
s = source
t = target
c = cold stream
d = disturbance
E = heat exchangers in the system
h = hot stream
max = control precision requirement
R = reduced vector or matrix for a system model
split = stream branches after splitting

Symbols

$\otimes$ = element multiplication operator
[1] = element value in $\boldsymbol{S}$ for an intermediate stream leaving a heat exchanger
{1} = element value in $\boldsymbol{S}$ for an intermediate stream entering a heat exchanger
$'$ = selected bypass
(lim) = upper limit of a bypass nominal fraction
$+$ = pseudo inverse of a matrix
$(+)$ = maximum positive fluctuation
$(-)$ = maximum negative fluctuation
$*$ = lumped system model

Literature Cited

Aguilera, N., and J. L. Marchetti, "Optimizing and Controlling the Operation of Heat-Exchanger Networks," *AIChE J.*, **44**, 1090 (1998).

Calandranis, J., and G. Stephanopoulos, "Structural Operability

Analysis of Heat Exchanger Networks," *Chem. Eng. Res. Des.*, **64**, 347 (1986).
Calandranis, J., and G. Stephanopoulos, "A Structural Approach to the Design of Control Systems in Heat Exchanger Networks," *Comput. Chem. Eng.*, **12**, 651 (1988).
Cao, Y., "Control Structure Selection for Chemical Processes Using Input-Output Controllability Analysis," PhD Thesis, Univ. of Exeter, Exeter, UK (1996).
Chang, J. W., and C. C. Yu, "Relative Disturbance Gain Array," *AIChE J.*, **38**, 521 (1992).
Colberg, R. D., and M. Morari, "Analysis and Synthesis of Resilient Heat Exchanger Networks," *Advances in Chemical Engineering*, Vol. 14, Academic Press, New York (1988).
Dolan, W. B., P. T. Cummings, and M. D. LeVan, "Heat Exchanger Network Design by Simulated Annealing," *Proc. First Int. Conf. on Foundation of Computer Aided Process Operation*, Park City, UT (1987).
Fisher, W. R., M. F. Doherty, and J. M. Douglas, "The Interface Between Design and Control. 1. Process Controllability," *Ind. Eng. Chem. Res.*, **27**, 597 (1988a).
Fisher, W. R., M. F. Doherty, and J. M. Douglas, "The Interface Between Design and Control. 2. Process Operability," *Ind. Eng. Chem. Res.*, **27**, 606 (1988b).
Fisher, W. R., M. F. Doherty, and J. M. Douglas, "The Interface Between Design and Control. 3. Selecting a Set of Controlled Variables," *Ind. Eng. Chem. Res.*, **27**, 611 (1988c).
Floudas, C. A., and I. E. Grossmann, "Synthesis of Flexible Heat Exchanger Networks for Multiperiod Operation," *Comput. Chem. Eng.*, **10**, 153 (1986).
Galli, M. R., and J. Cerda, "Synthesis of Flexible Heat Exchanger Networks—III: Temperature and Flowrate Variations," *Comput. Chem. Eng.*, **15**, 7 (1991).
Huang, Y. L., and L. T. Fan, "HIDEN: A Hybrid Intelligent System for Synthesizing Highly Controllable Exchanger Networks: Implementation of Distributed Strategy for Integration of Process Design and Control," *Ind. Eng. Chem. Res.*, **33**, 1174 (1994).
Kotjabasakis, E., and B. Linnhoff, "Sensitivity Tables for the Design of Flexible Processes (1)—How Much Contingency in Heat Exchanger Network is Cost-Effective?" *Chem. Eng. Res. Des.*, **64**, 197 (1986).
Linnhoff, B., and E. Kotjabasakis, "Downstream Paths for Operable Process Design," *Chem. Eng. Prog.*, **82**(5), 23 (1986).
Mathisen, K. W., S. Skogestad, and E. A. Wolff, "Controllability of Heat Exchanger Networks," AIChE Meeting, Los Angeles, CA (1991).
Mathisen, K. W., S. Skogestad, and T. Gundersen, "Optimal Bypass Placement in Heat Exchanger Networks," AIChE Meeting, New Orleans, LA (1992).
Mathisen, K. W., M. Morari, and S. Skogestad, "Optimal Operation of Heat Exchanger Networks," *Proc. PSE '94*, E. S. Yoon, ed., Korean Inst. of Chemical Engineers, Korea, p. 315 (1994).
McAvoy, T. J., "Integration of Process Design and Process Control," *Recent Development in Chemical Process and Plant Design*, Y. A. Liu, H. A. McGee, Jr., and W. R. Epperly, eds., Wiley, New York, p. 289 (1987).
Morari, M., "Flexibility and Resilience of Process Systems," *Comput. Chem. Eng.*, **7**, 423 (1983).
Morari, M., "Effect of Design on the Controllability of Chemical Plants," *Proc. IFAC Workshop on Interactions Between Process Design and Process Control*, London, p. 3 (1992).
Nobel, B., and J. W. Daniel, *Applied Linear Algebra*, 2nd ed., Prentice-Hall, Englewood Cliffs, NJ (1977).
Papalexandri, K. P., and E. N. Pistikopoulos, "A Multiperiod MINLP Model for the Synthesis of Flexible Heat and Mass Exchange Network," *Comput. Chem. Eng.*, **18**, 1125 (1994a).
Papalexandri, K. P., and E. N. Pistikopoulos, "Synthesis and Retrofit Design of Operable Heat Exchanger Network: 1. Flexibility and Structural Controllability Aspects," *Ind. Eng. Chem. Res.*, **33**, 1718 (1994b).
Papoulias, S. A., and I. E. Grossmann, "A Structural Optimization Approach in Process Synthesis-II. Heat Recovery Networks," *Comp. Chem. Eng.*, 7 (1983).
Saboo, A. K., M. Morari, and D. C. Woodcock, "Design of Resilient Processing Plants—III: A Resilience Index for Heat Exchanger Networks," *Chem. Eng. Sci.*, **40**, 1553 (1985).
Skogestad, S., and I. Postlethwaite, "Multivariable Feedback Control—Analysis and Design," Wiley, Chichester, UK (1996).
Uzturk, D., and U. Akman, "Centralized and Decentralized Control of Retrofit Heat-Exchanger Networks," *Comput. Chem. Eng.*, **21**, S373 (1997).
Yan, Q. Z., and Y. L. Huang, "Extended Disturbance Propagation Model for Designing an Optimal Heat Exchanger Network with Bypass Under Uncertainty," AIChE Meeting, Miami, FL (1998).
Yan, Q. Z., and Y. L. Huang, "Cost-Effective Disturbance Rejection: Design of a Heat Exchanger Network with Bypasses Using a Disturbance Propagation and Control Model," *AIChE Meeting*, Dallas, TX (1999).
Yang, Y. H., "Mode-Based Integration of Process Design and Control via Process Synthesis: Application to the Development of Highly Controllable and Environmentally Benign Processes," PhD Diss., Wayne State Univ., Detroit, MI (1999).
Yang, Y. H., J. P. Gong, and Y. L. Huang, "A Simplified System Model for Rapid Evaluation of Disturbance Propagation through a Heat Exchanger Network," *Ind. Eng. Chem. Res.*, **35**, 4550 (1996).
Yang, Y. H., H. H. Lou, and Y. L. Huang, "Steady-State Disturbance Propagation Modeling of Heat Integrated Distillation Processes," *Trans. Inst. Chem. Eng.*, Part A, **78**, 245 (2000).
Yang, Y. H., Q. Z. Yan, and Y. L. Huang, "A Unified Model for the Prediction of Structural Disturbance Propagation in Mass Exchanger Networks," *Trans. Inst. Chem. Eng.*, Part A, **77**, 253 (1999).
Yee, T. F., and I. E. Grossmann, "Simultaneous Optimization Models for Heat Integration—II, Heat Exchanger Networks Synthesis," *Comput. Chem. Eng.*, **10**, 1165 (1990).

Appendix A: HEN Structural Representation

The construction of structural matrix $\boldsymbol{S}$ and the derivation of conversion matrices $\boldsymbol{V}_1$ through $\boldsymbol{V}_3$ are demonstrated using the example in Figure A1. In this example, the HEN has a hot stream and two cold streams connected by two heat exchangers (HEXs). Matrix $\boldsymbol{S}$ has a dimension of 4×4 (that is, $2N_e\times2N_e$). It is decomposed into two submatrices, $\boldsymbol{S}_1$ (3×4) and $\boldsymbol{S}_2$ (1×4), respectively.

Construction of $\boldsymbol{S}_1$. In submatrix $\boldsymbol{S}_1$, three rows are designated to streams H_1, C_1, and C_2 in sequence. The four columns are divided into two pairs: the left pair is for exchanger E_1, and the right is for exchanger E_2. This submatrix

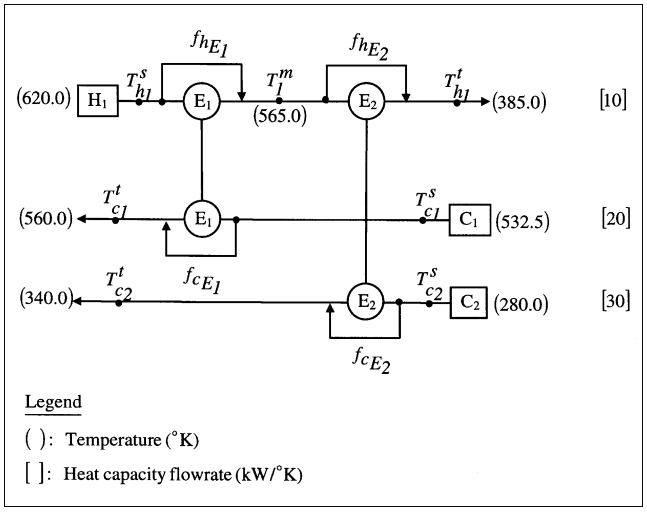

Figure A1. HEN structure with bypasses as manipulated variables to control target temperatures.

is developed as follows:

$$\boldsymbol{S}_1 = \begin{array}{c} \\ H_1^{\text{in}} \\ C_1^{\text{out}} \\ C_2^{\text{out}} \end{array} \begin{array}{c} \overbrace{\begin{array}{cc} h & c \end{array}}^{E_1} \quad \overbrace{\begin{array}{cc} h & c \end{array}}^{E_2} \\ \begin{pmatrix} 1 & 0 & 1 & 0 \\ 0 & 1 & 0 & 0 \\ 0 & 0 & 0 & 1 \end{pmatrix} \end{array} \begin{array}{c} H_1^{\text{out}} \\ C_1^{\text{in}} \\ C_2^{\text{in}} \end{array}. \tag{A1}$$

In the submatrix, each row from the left to the right stands for the stream temperature from the hot end to the cold end. For instance, the left side of the first row is for the inlet of hot stream H_1 (that is, H_1^{in}) and the right side is for the outlet of the same stream (that is, H_1^{out}). In each pair of columns, the left and the right column are assigned to the hot stream and the cold stream going through the HEX, respectively. An element having a value of 1 or 0 means the stream going through or not going through the HEX. For example, the first row is the vector of (1 0 1 0). This indicates that hot stream H_1 enters E_1 and E_2. The second row has the vector of (0 1 0 0). This means that stream C_1 enters E_1.

Construction of S_2. In submatrix $\boldsymbol{S}_2$, each row is designated to an intermediate stream. For this example there is only one intermediate stream, M_1, which is between exchangers E_1 and E_2. The definition of columns is the same as that in submatrix $\boldsymbol{S}_1$. Figure A1 shows that the intermediate stream leaves E_1 and enters E_2. Thus, the first and third elements of S_2 are set to {1} and [1], respectively. The submatrix is

$$\boldsymbol{S}_2 = M_1 \left(\overbrace{\begin{array}{cc} h & c \end{array}}^{E_1} \quad \overbrace{\begin{array}{cc} h & c \end{array}}^{E_2} \right) \\ \{1\} \quad 0 \quad [1] \quad 0 \big). \tag{A2}$$

Note that an element having a value of 0 means that the intermediate stream does not go through the HEX at the side specified.

By combining submatrices $\boldsymbol{S}_1$ and $\boldsymbol{S}_2$, the following structural matrix $\boldsymbol{S}$ can be obtained:

$$\boldsymbol{S} = \begin{pmatrix} \boldsymbol{S}_1 \\ \boldsymbol{S}_2 \end{pmatrix} = \begin{pmatrix} 1 & 0 & 1 & 0 \\ 0 & 1 & 0 & 0 \\ 0 & 0 & 0 & 1 \\ \{1\} & 0 & [1] & 0 \end{pmatrix}. \tag{A3}$$

Derivation of V_1. Matrix V_1 has the same dimension as matrix $\boldsymbol{S}$ (4×4). Each column j ($j = 1, 2, \ldots, 4$) in V_1 is generated based on the same column in $\boldsymbol{S}$. For the first column in $\boldsymbol{S}$, since $s_{4,1}$, is {1}, then $v_{1_{4,1}}$ should be equal to 1 and all three other elements in the same column be 0. As $s_{4,3}$ in $\boldsymbol{S}$ is [1], then $v_{1_{4,3}}$ needs to be equal to 0 and $v_{1_{i,3}}$ is equal to $s_{i,3}$ ($i = 1, 2, 3$). Since the other two columns ($j = 2, 4$) in $\boldsymbol{S}$ don't contain {1} and [1], $v_{1_{i,j}}$ should be equal to $s_{i,j}$ ($i = 1, 2, \ldots, 4$). Hence, the resultant V_1 is

$$\boldsymbol{V}_1 = \begin{pmatrix} 0 & 0 & 1 & 0 \\ 0 & 1 & 0 & 0 \\ 0 & 0 & 0 & 1 \\ 1 & 0 & 0 & 0 \end{pmatrix}. \tag{A4}$$

Derivation of V_2. Matrix V_2 also has the dimension of 4×4. Each row j is generated based on the same column in matrix $\boldsymbol{S}$. As $s_{4,1}$ in $\boldsymbol{S}$ is {1}, $v_{2_{1,4}}$ needs to be 0, and $v_{2_{1,4}}$ to be $s_{i,1}$ ($i = 1, 2, 3$). Since $s_{4,3}$ in $\boldsymbol{S}$ is [1], $v_{2_{3,4}}$ should be 1 and $v_{2_{3,i}}$ should be 0 ($i = 1, 2, 3$). The other two columns ($j = 2, 4$) in $\boldsymbol{S}$ don't contain {1} or [1], so $v_{2_{i,i}}$ should be $s_{i,j}$ ($i = 1, 2, \ldots, 4$). Therefore, the resultant V_2 is

$$\boldsymbol{V}_2 = \begin{pmatrix} 1 & 0 & 0 & 0 \\ 0 & 1 & 0 & 0 \\ 0 & 0 & 0 & 1 \\ 0 & 0 & 1 & 0 \end{pmatrix}. \tag{A5}$$

Derivation of V_3. Matrix V_3 has the dimension of 4×3. Since each column of matrix $\boldsymbol{S}$ contains at most one {1} or one [1], we can let $v_{3_{j,i}}$ equal $s_{i,j}$ ($i = 1, 2, 3$; $j = 1, 2, \ldots, 4$). Thus, the resultant V_3 is

$$\boldsymbol{V}_3 = \begin{pmatrix} 1 & 0 & 0 \\ 0 & 1 & 0 \\ 1 & 0 & 0 \\ 0 & 0 & 1 \end{pmatrix} \tag{A6}$$

Appendix B: Two Key Theorems from Nobel and Daniel (1977)

Theorem 1: Identification of the Pseudoinverse of a Non-squared Matrix. Let matrix $\boldsymbol{B}$ ($N_s \times 2N_e$) of rank k have the following singular value decomposition:

$$\underline{\boldsymbol{B}} = \boldsymbol{U} \Sigma \boldsymbol{V}^{\boldsymbol{T}}, \tag{B1}$$

where

$$\boldsymbol{\Sigma} = \begin{pmatrix} \boldsymbol{E} & \boldsymbol{0} \\ \boldsymbol{0} & \boldsymbol{0} \end{pmatrix} \tag{B2}$$

$$\boldsymbol{E} = \text{diag}\{\sigma_1, \sigma_2, \ldots, \sigma_k\}, \tag{B3}$$

and

$$\sigma_1 \geq \sigma_2 \geq \cdots \geq \sigma_k > 0, \tag{B4}$$

where $\boldsymbol{U}$, $\boldsymbol{\Sigma}$, and $\boldsymbol{V}$ have dimensions of $N_s \times N_s$, $N_s \times 2N_e$, and $2N_e \times 2N_e$, respectively. The pseudoinverse, $\underline{\boldsymbol{B}}^+$, of $\underline{\boldsymbol{B}}$ can be calculated as

$$\underline{\boldsymbol{B}}^+ = \boldsymbol{V} \boldsymbol{\Sigma}^+ \boldsymbol{U}^{\boldsymbol{T}}, \tag{B5}$$

where

$$\boldsymbol{\Sigma}^+ = \begin{pmatrix} \boldsymbol{E}^{-1} & \boldsymbol{0} \\ \boldsymbol{0} & \boldsymbol{0} \end{pmatrix}. \tag{B6}$$

Theorem 2: Identification of the Optimal Solution of Eq. 66. For matrix $\underline{\boldsymbol{B}}$ ($N_s \times 2N_e$, and $2N_e$) of rank k with the singular-value decomposition shown in Eq. B1, the solution $\boldsymbol{\delta f}'$ ($N_{f'} \times 1$) that minimizes $\| \underline{\boldsymbol{B}} \boldsymbol{V}_4 \boldsymbol{\delta f}' - \boldsymbol{d} \|_2$ can be expressed as

$$\boldsymbol{V}_4 \boldsymbol{\delta f}' = \boldsymbol{V} \boldsymbol{W}, \tag{B7}$$

where V_4 $(2N_e \times N_{f'})$ is defined in Eq. 62, V $(2N_e \times N_s)$ is defined in Eq. B1, and the elements of W $(N_s \times 1)$ are defined as

$$w_i = \begin{cases} \dfrac{b'_i}{\sigma_i} & i = 1, 2, \ldots, k \\ 0 & i = k+1, k+2, \ldots, N_s, \end{cases} \tag{B8}$$

where b'_i is an element in the following matrix:

$$\boldsymbol{b}' = \boldsymbol{U}^T \boldsymbol{d}, \tag{B9}$$

and σ_i is defined in Eqs. B2 through B4.

Appendix C: Derivation of the Upper Limits of Bypass Fractions

Equations 77 and 78 are derived based on the requirement of minimum temperature driving force ($\Delta T_{\min}$) for a HEX. Referring to Figure 1, the following relationships must hold:

$$T_h^i - T_c^o \geq \Delta T_{\min} \tag{C1}$$

$$T_h^o - T_c^i \geq \Delta T_{\min}. \tag{C2}$$

Note that

$$T_h^i - T_c^o = T_h^s - T_c^o \tag{C3}$$

$$T_h^o - T_c^i = T_h^o - T_c^s. \tag{C4}$$

According to Eq. 18, we have the following relationship for the bypass placed on the hot-stream side of the HEX:

$$T_h^t = f_h T_h^s + (1 - f_h) T_h^o. \tag{C5}$$

Similarly, the relationship for the bypass placed on the cold-stream side of the HEX is

$$T_c^t = f_c T_c^s + (1 - f_c) T_c^o \tag{C6}$$

Substituting Eqs. C4 and C6 into Eq. C2 and rearranging the resultant equation yield,

$$T_h^t - T_c^s - \Delta T_{\min} \geq f_h (T_h^s - T_c^s - \Delta T_{\min}). \tag{C7}$$

Since the term $T_h^s - T_c^s - \Delta T_{\min}$ is definitely positive, it becomes

$$f_h \leq \frac{T_h^t - T_c^s - \Delta T_{\min}}{T_h^s - T_c^s - \Delta T_{\min}}. \tag{C8}$$

In other words, the upper limit of the nominal fraction of the bypass placed on the hot-stream side of a HEX, $f_h^{(\lim)}$, is

$$f_h^{(\lim)} = \frac{T_h^t - T_c^s - \Delta T_{\min}}{T_h^s - T_c^s - \Delta T_{\min}}. \tag{C9}$$

Following the same approach, we can obtain the following upper limit of the nominal fraction of the bypass placed on the cold-stream side of a HEX:

$$f_c^{(\lim)} = \frac{T_h^s - T_c^t - \Delta T_{\min}}{T_h^s - T_c^s - \Delta T_{\min}}. \tag{C10}$$

Appendix D: Calculation of an Extended RGA

An extended RGA can be derived using the Nobel and Daniel theorems cited in Appendix B. In this work, an optimal solution for nominal values of selected bypass $\underline{\delta f'}$ is sought, that is,

$$\min_{\underline{\delta f'}} \| \underline{\boldsymbol{B}} \boldsymbol{V}_4 \underline{\delta f'} - \boldsymbol{d} \|_2. \tag{D1}$$

According to their theorems, the matrix in Eq. 88, that is, the control matrix $\boldsymbol{B}$ is

$$\underline{\boldsymbol{B}} = \begin{pmatrix} 86.3 & 43.1 & 0 & 0 & 0 & 0 \\ -14.1 & -7.05 & 31.0 & 23.3 & 28.8 & 14.4 \\ -22.8 & -11.4 & -44.8 & -33.6 & 0 & 0 \\ -6.5 & -3.25 & 14.3 & 10.7 & -14.4 & -7.2 \end{pmatrix}. \tag{D2}$$

The singular decomposition analysis is

$$\boldsymbol{U} = \begin{pmatrix} 0.941 & -0.148 & 0.179 & -0.248 \\ -0.117 & 0.658 & 0.644 & -0.372 \\ -0.315 & -0.713 & 0.384 & -0.495 \\ -0.045 & 0.194 & -0.637 & -0.745 \end{pmatrix} \tag{D3}$$

$$\boldsymbol{\Sigma} = \begin{pmatrix} 101.7 & 0 & 0 & 0 & 0 & 0 \\ 0 & 71.6 & 0 & 0 & 0 & 0 \\ 0 & 0 & 32.0 & 0 & 0 & 0 \\ 0 & 0 & 0 & 0.011 & 0 & 0 \end{pmatrix} \tag{D4}$$

$$\boldsymbol{V} = \begin{pmatrix} 0.888 & -0.098 & 0.053 & -0.447 & 0 & 0 \\ 0.443 & -0.049 & 0.026 & 0.895 & 0 & 0 \\ 0.097 & 0.769 & -0.198 & 0 & -0.6 & 0 \\ 0.073 & 0.577 & -0.147 & 0 & 0.8 & 0 \\ -0.027 & 0.225 & 0.865 & 0 & -0.001 & -0.447 \\ -0.013 & 0.113 & 0.433 & 0 & -0.001 & 0.894 \end{pmatrix} \tag{D5}$$

Because the fourth singular value, σ_4 (0.011), is much smaller compared with the first three, it is regarded as zero according to the Nobel and Daniel theorem and condition.

For the first example,

$$\boldsymbol{\Sigma}^+ = \begin{pmatrix} 0.0098 & 0 & 0 & 0 & 0 & 0 \\ 0 & 0.014 & 0 & 0 & 0 & 0 \\ 0 & 0 & 0.0312 & 0 & 0 & 0 \\ 0 & 0 & 0 & 0 & 0 & 0 \end{pmatrix}. \tag{D6}$$

The pseudoinverse of $\boldsymbol{B}$ can be calculated according to Eq. B5

$$\underline{\boldsymbol{B}}^{+} = \boldsymbol{V} \cdot \boldsymbol{\Sigma}^{+} \cdot \boldsymbol{U}^{\mathbf{T}}$$

$$= \begin{pmatrix} 0.0087 & -0.0009 & -0.0011 & -0.0017 \\ 0.0043 & -0.0004 & -0.0006 & -0.0009 \\ -0.0018 & 0.0030 & -0.0103 & 0.0060 \\ -0.0013 & 0.0023 & -0.0077 & 0.0045 \\ 0.0041 & 0.0195 & 0.0082 & -0.0166 \\ 0.0021 & 0.0097 & 0.0041 & -0.0083 \end{pmatrix}. \quad \text{(D7)}$$

Then, RGA can be calculated using the formula in Eq. 68:

$$\boldsymbol{\Lambda} = \underline{\boldsymbol{B}} \otimes \underline{\boldsymbol{B}}^{+}$$

$$= \begin{pmatrix} 0.7512 & 0.1873 & 0 & 0 & 0 & 0 \\ 0.0120 & 0.0030 & 0.0920 & 0.0526 & 0.5613 & 0.1403 \\ 0.0259 & 0.0065 & 0.04625 & 0.2597 & 0 & 0 \\ 0.0111 & 0.0028 & 0.0855 & 0.0477 & 0.2387 & 0.0597 \end{pmatrix}. \quad \text{(D8)}$$

Manuscript received May 3, 1999, and revision received Feb. 14, 2000.